Chapter 15
Climate Change in Southern South America During the Last Two Millennia

Christopher M. Moy, Patricio I. Moreno, Robert B. Dunbar, Michael R. Kaplan, Jean-Pierre Francois, Ricardo Villalba, and Torsten Haberzettl

Abstract Paleoclimate records from southern South America can be used to address important questions regarding the timing and nature of late-Holocene climate variability. During the last 30 years, many areas of southern South America have experienced rapid climatic and ecological changes that are driven by global and hemispheric-scale ocean-atmosphere processes. In order to place these recent changes in a longer-term context, we first present an overview of the modern climate processes relevant for the interpretation of paleoclimate records in southern South America, and then review records that have been developed from various archives that span the last two thousand years. Multiple paleoclimate records provide evidence for an overall decrease in temperature and an increase in westerly wind intensity that culminates in the last few hundred years during the time of the European Little Ice Age. We also find evidence for aridity generally coincident with the Medieval Climate Anomaly in several paleoclimate archives. Although much work has been done in this region, high-resolution well-dated archives are still needed from sensitive locations to improve our understanding of past and present climate change. From the paleoclimate records that we have compiled, we infer that warming, retreat of glaciers, and reconfiguration of precipitation patterns during the past century is unique within the context of the last 2000 years.

Keywords South America · Patagonia · Paleoclimate · Southern Hemisphere Westerlies · Little Ice Age

15.1 Introduction

Southernmost South America is an important venue for examining the timing and nature of past climate change. The region of Patagonia including Tierra del Fuego spans ~15° of latitude and represents the southernmost continuous landmass outside

C.M. Moy (✉)
Department of Geological and Environmental Sciences, 450 Serra Mall, Braun Hall (Bldg. 320), Stanford University, Stanford, CA 94305-2115 USA
e-mail: moyc@stanford.edu

F. Vimeux et al. (eds.), *Past Climate Variability in South America and Surrounding Regions*, Developments in Paleoenvironmental Research 14,
DOI 10.1007/978-90-481-2672-9_15,

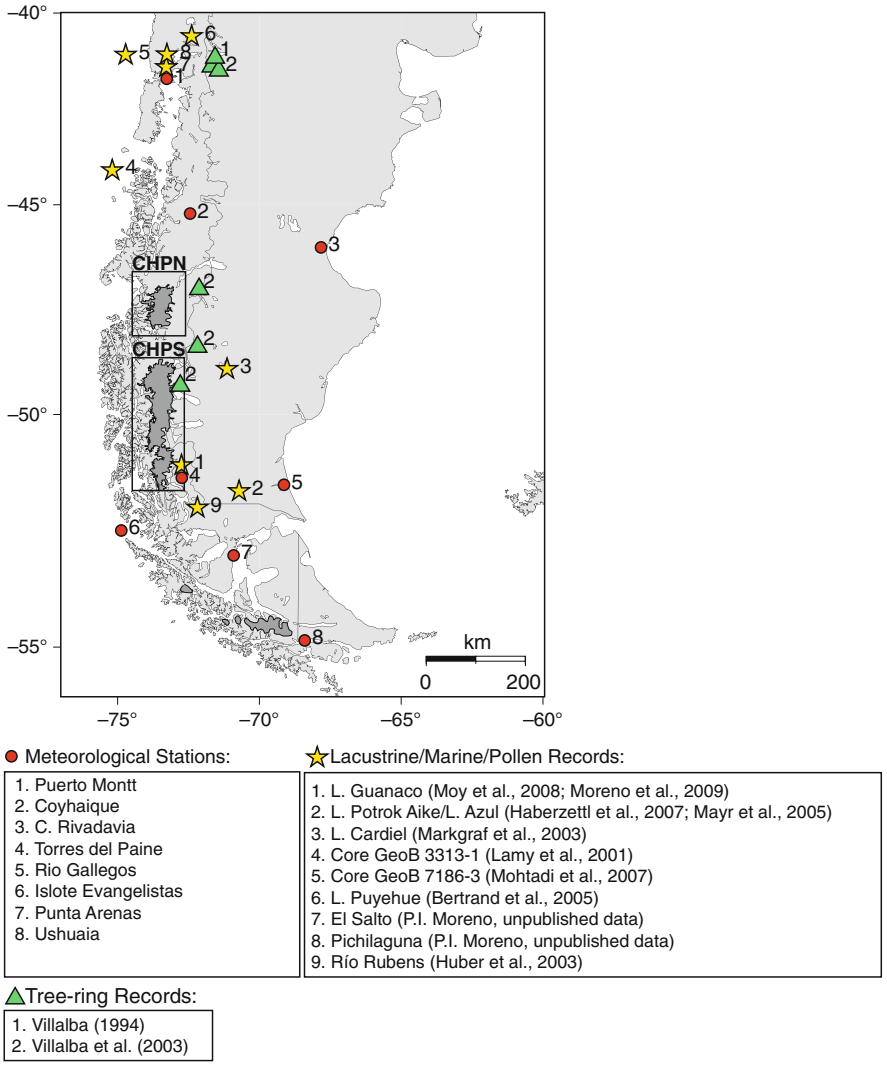

Fig. 15.1 Map of southern South America highlighting meteorological stations and the locations of paleoclimate records referenced in this paper. The black rectangle highlights the modern ice extent (*grey* regions) of the Campo de Hielo Patagónico Norte (CHPN) and Sur (CHPS) or northern and southern Patagonian ice fields

of Antarctica (Fig. 15.1). The N-S oriented Andes have an average elevation of 2500 m in southern South America, and are a significant topographical divide that establishes sharp climate and vegetation gradients from west to east. The geography and climate of southern South America support a diverse array of natural climate archives, such as glaciers and ice caps, tree rings, and lake sediments that can be used to better understand how climate has changed in the past.

The present-day climate of the region is influenced by processes that originate in the high latitudes and the tropics, most notably the Southern Annual Mode (SAM) or the Antarctic Oscillation (AAO) and the El Niño-Southern Oscillation (ENSO). Both of these large-scale ocean-atmosphere processes play a role in altering not only temperatures at seasonal to interannual timescales, but also precipitation amount and distribution through changes in the strength and latitudinal position of the southern westerlies (Garreaud et al. 2008). Southern South America is unique in that it is the only large landmass that extends through the core of the modern westerly wind field at ~50°S (Fig. 15.2) permitting the study of past westerly wind variability using terrestrial climate archives.

The modern instrumental record of temperature and precipitation in Patagonia is short (typically less than 50 years), discontinuous, and spatially limited. Despite these shortcomings, modern observations suggest patterns that are of paleoclimate significance. Over the last 30 years, a strengthening of atmospheric circulation in the high southern latitudes is evident in direct instrumental observations (Marshall 2003) and wind fields derived from reanalysis data sets (Thompson and Wallace 2000), reflecting a trend towards the positive mode or phase of the SAM. An increase in summer air temperature in southern Patagonia, concurrent with a decrease in summer temperatures in coastal areas in northern Patagonia, is observed during the same period (Carrasco et al. 2008, Villalba et al. 2003). The trend in the SAM towards positive index values has significant implications for the global carbon cycle, in particular the rates of CO_2 exchange between the ocean and atmosphere in the high southern latitudes (Canadell et al. 2007, Le Quéré et al. 2007, Lovenduski et al. 2007). The regional pattern of summer warming and cooling in recent decades has implications for understanding the mechanisms of past, present, and future climate change.

In addition to modern climate change observed in instrumental records, paleoclimate records provide evidence of climate variations during the last 2000 years. For instance, there have been significant changes in ENSO event frequency and magnitude in the tropics during the last 2000 years (Cobb et al. 2003, Moy et al. 2002, Rein et al. 2004). Within the last 1000 years, Northern Hemisphere climatic events such as the Little Ice Age (LIA), from 380 to 50 calendar years before present (cal year BP, where 1950 = 0 cal year BP) (Matthews and Briffa 2005), and the Medieval Climate Anomaly (MCA), between 950 and 750 cal year BP, have been identified in paleoclimate records throughout both hemispheres (Stine 1994). However, these events are regionally complex (Bradley et al. 2003, Jones and Mann 2004) and their timing, magnitude, and nature have not been clearly delineated in southern South America. In addition, changes in glacial ice extent evident in both the northern and southern Patagonian ice fields are related to Neoglaciation, which has been recognized throughout the Southern Hemisphere, beginning ~5400 cal year BP and ending with the recent retreat from LIA ice positions (Clapperton and Sugden 1988, Hodell et al. 2001, Porter 2000, Schaefer et al., 2009). These climatic events and trends set the stage for our understanding of climate variability during the last 2000 years.

Here, we review the record of paleoclimate change in Patagonia during the last 2000 years. We first present an overview of the modern climate of the region and

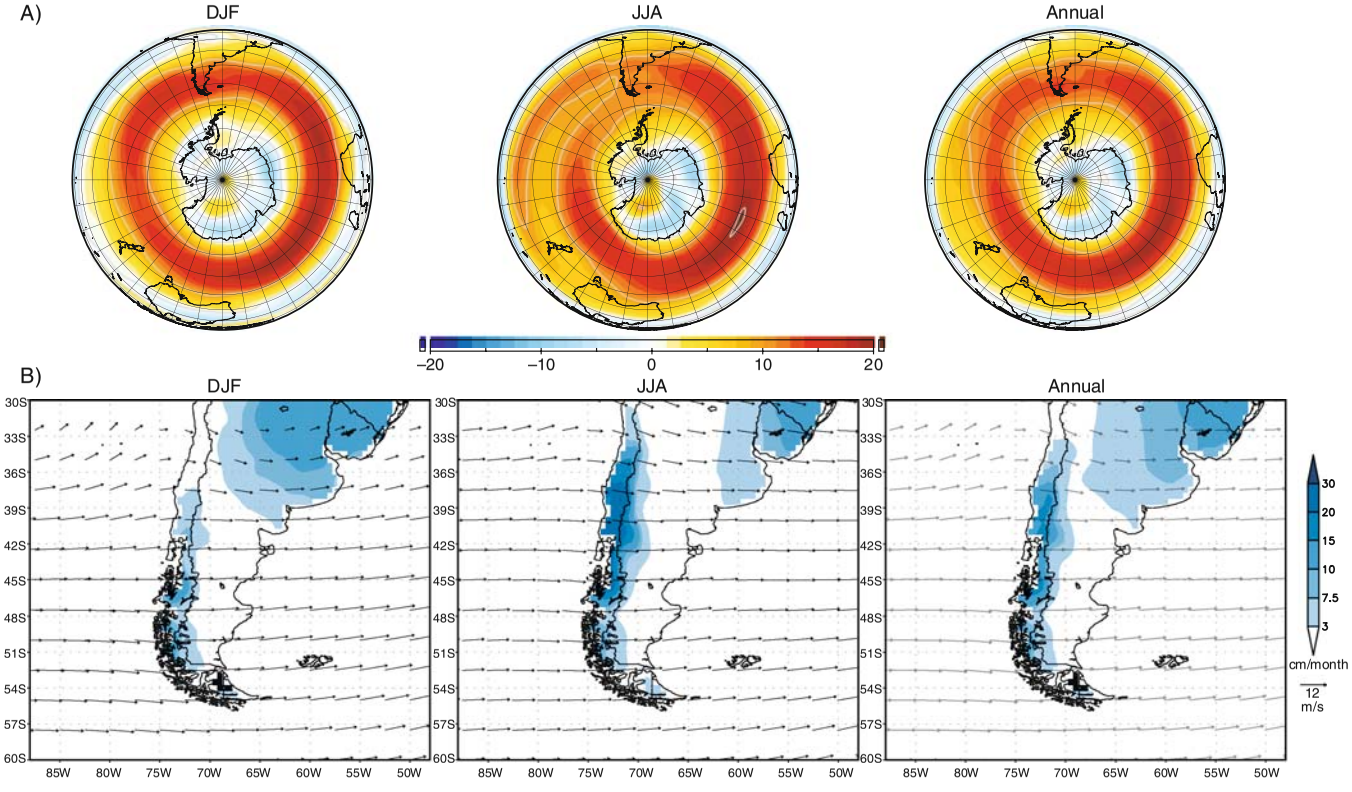

Fig. 15.2 Annual and seasonal composite means of atmospheric circulation and precipitation in southern South America from 1980 to 2006. (**A**) Summer (DJF), winter (JJA), and annual composite averages of 700 hPa zonal wind speed (m/s) from the NCEP-NCAR reanalysis. During DJF the westerlies are strongest and shifted poleward over southern Patagonia, which is in contrast to the winter months (JJA), which exhibit reduced wind strength and northward expansion of the wind field. (**B**) summer (DJF), winter (JJA), and annual composite averages of U. Delaware surface precipitation rate (cm/month) and 700 hPa wind vectors in southern South America. The 700 hPa wind vectors (reference arrow at right of plot) show strong westerly flow during all seasons in southern South America. Note that the location of maximum precipitation in (**B**) follows the seasonal migration of the 700 hPa westerly wind maximum in (**A**)

focus on the interannual linkages between tropical and high-latitude forcing mechanisms that are important for the interpretation of paleoclimate records. We then present results from a lake sediment record from Lago Guanaco, which is located within the modern westerly wind maximum (∼50°S), and highlight late-Holocene changes in moisture balance related to the westerlies. We incorporate existing paleoclimate records from Patagonia, which include lake sediment, pollen and charcoal, geomorphologic (glacial and lake level), tree-ring, and marine data in order to answer the following questions:

1. Can we identify global climate events (such as the Northern LIA and MCA) in southern South America? If so, is the timing and nature of these past changes synchronous and of the same sign/direction throughout Patagonia?
2. How has the strength and latitudinal position of the Southern Hemisphere westerly wind field changed during the last 2000 years? Can we identify trends in climate or climate variability that place the modern conditions in perspective?
3. What are potential forcing mechanisms of climate change in southernmost South America at centennial and millennial timescales? Are there links between past climate variability observed in this region with both tropical and high-latitude records of climate change during the last 2000 years?

15.2 Climatology

To place paleoclimate records in a proper context, we provide a brief summary of present-day climate, including the general atmospheric circulation, the relationship between wind and precipitation, seasonal and interannual variability, and potential tropical and high latitude forcing mechanisms. We focus on interactions between atmospheric circulation and precipitation because the two often exhibit strong correlations in southern South America, and this modern link between precipitation and zonal atmospheric flow is commonly used in paleoclimate studies to identify past changes in the intensity and latitudinal position of the westerlies. More extensive reviews on extratropical climate variability in South America, which discuss variations in the thermal and precipitation fields, can be found in Garreaud and Aceituno (2007) and Garreaud et al. (2008).

15.2.1 Co-Variability of Wind and Precipitation

Southern South America is an excellent place to investigate past variations in the Southern Hemisphere westerlies for three reasons: First, it is the only significant continental landmass that intersects the region of maximum zonal flow in the Southern Hemisphere (Fig. 15.2). The strongly oceanic nature of the mid- to high southern latitudes leads to the high zonal symmetry observed in both lower and upper level zonal wind on monthly to interannual timescales. One advantage of this zonal structure is that a meridional transect through the core of the westerlies at a given location has relevance across a range of longitudes.

Second, atmospheric circulation in the southern mid-latitudes is maintained by strong thermal gradients in the troposphere and in sea-surface temperatures (SST) over the Pacific Ocean. The strong atmospheric pressure gradient drives geostrophic flow and promotes baroclinic instability and the formation of transient eddies (Garreaud and Aceituno 2007). These eddies in turn produce frontal systems in the form of migratory surface cyclones and anticyclones that drift eastward and are "steered" by the 700 hPa winds along storm tracks located poleward of the upper-level jet (Garreaud 2007, Trenberth 1991). Increasing wind intensity or strength of zonal flow increases baroclinic instability, which increases the succession of extratropical cyclones circling the Southern Ocean and impinging on the South American continent (Garreaud 2007).

Third, topography and the general circulation are closely related in that the southern Andes are the only formidable obstacle to tropospheric flow in the Southern Hemisphere. The uplift of air over the cordillera produces significant amounts of orographic precipitation (>10000 mm/year), while farther to the east, subsidence produces an overall drying effect in Argentine Patagonia and the Atlantic seaboard (Garreaud et al. 2008). Orographic precipitation on the windward side of the Andes increases with both altitude and overall westerly wind strength to produce extreme environmental and climatological gradients. For example, at 50°S, annual precipitation ranges from 3000 mm/year at western coastal sites, to 6000 mm/year at sea level on the western slope of the Andes, to an estimated 8000–10000 mm/year along the crest of the cordillera, rapidly decreasing to less that 500 mm/year east of Punta Arenas and 200–300 mm/year on the Atlantic seaboard (Garreaud et al. 2008, Schneider et al. 2003, Villalba et al. 2003). At lat. 41°S, annual precipitation ranges from 1800 mm/year in Puerto Montt, up to 4000 mm/year on the continental divide, and falls to less than 1000 mm/year in Bariloche (Villalba et al. 2003).

15.2.2 Seasonal Variations in Wind and Precipitation

Figure 15.2 displays the annual cycle of precipitation and low-level winds (700 hPa) in southern South America. We use the University of Delaware global precipitation data set derived from surface instrumental data from the NOAA GHCN network and the climate archive compiled by Legates and Willmott (1990). Wind vectors represent the long-term mean of annual, summer, and winter wind magnitude and direction at 700 hPa derived from the NCEP-NCAR reanalysis (Kalnay et al. 1996). During the austral summer (DJF), low level winds are strongest and situated in their most poleward or southern position of the year at approximately 50°S (Fig. 15.2). During austral winter (JJA), the low-level winds weaken, especially in Southern Patagonia, and the main axis of the wind field migrates north. The northward migration is mainly due to seasonal changes in SST and the northward migration of the anticyclonic high pressure cell situated in the southeastern Pacific Ocean. Through the seasonal cycle, the main locus of precipitation largely follows the mean zonal wind maximum (Fig. 15.2). In southern Patagonia, precipitation is more evenly distributed throughout the year with a small maximum during the Austral autumn. In

contrast, precipitation in northern Patagonia is more seasonal with higher amounts during JJA when the subtropical high and the jet are located farther to the north (Fig. 15.2).

15.2.3 Correlation Between Zonal Wind and Precipitation

To highlight the relationship between precipitation and wind in southern South America, we calculate the annual spatial correlation between precipitation derived from 8 meteorological stations and the zonal wind at 700 hPa from the NCEP-NCAR reanalysis (Fig. 15.3). Monthly precipitation values for the selected locations were obtained from the NOAA GHCN, Dirección Meteorológica de Chile, Dirección General de Aguas, and the Servicio Hidrográfico de la Armada de Chile (SHOA) for the period from 1980 to 2003 (Table 15.1). We selected this 23 year period because the meteorological stations have good data coverage and it postdates the inclusion of satellite sounder data into the NCEP-NCAR reanalysis (Marshall 2003). Precipitation at Puerto Montt, Coyhaique, Torres del Paine and Islote Evangelistas exhibit an overall positive correlation with zonal wind speed that extends throughout much of the Southern Hemisphere, indicating that precipitation at annual timescales at a particular site is related to the atmospheric circulation over a significant portion of the Southern Hemisphere. The positive correlation extends to locations on the eastern side of the range: precipitation falling at Coyhaique and Torres del Paine exhibits significant positive correlations with the westerlies similar to I. Evangelistas, which is the westernmost site. The latitude of maximum positive correlation varies with location. For example, the correlation between precipitation and wind at Puerto Montt is most positive at ~40°S, reflecting the seasonal delivery of precipitation during the austral winter when the westerlies are shifted to the north. Two of the eastern Atlantic coastal locations, Comodoro Rivadavia and Río Gallegos, exhibit either negative or little correlation between zonal wind and precipitation, and this may reflect contribution of precipitation from the Atlantic Ocean. Mayr et al. (2007) present meteorological data from a station close to Laguna Potrok Aike, which is located in the Argentine steppe midway between the Andean divide and Río Gallegos on the Atlantic coast. There, higher rainfall is associated with easterly winds and the greater input of Atlantic moisture when the zonal westerlies are weak.

15.2.4 El Niño-Southern Oscillation (ENSO) Variability

ENSO plays a role in driving interannual climate variability in southern South America. NCEP reanalysis data indicate high annual correlations between a multivariate ENSO index (Wolter and Timlin 1993, Wolter and Timlin 1998) and zonal wind speed, precipitation and surface air temperature from 1980 to 2006 (Fig. 15.4). When averaged over the year, an ENSO warm event (positive multivariate ENSO index values) is associated with an overall decrease in the strength of

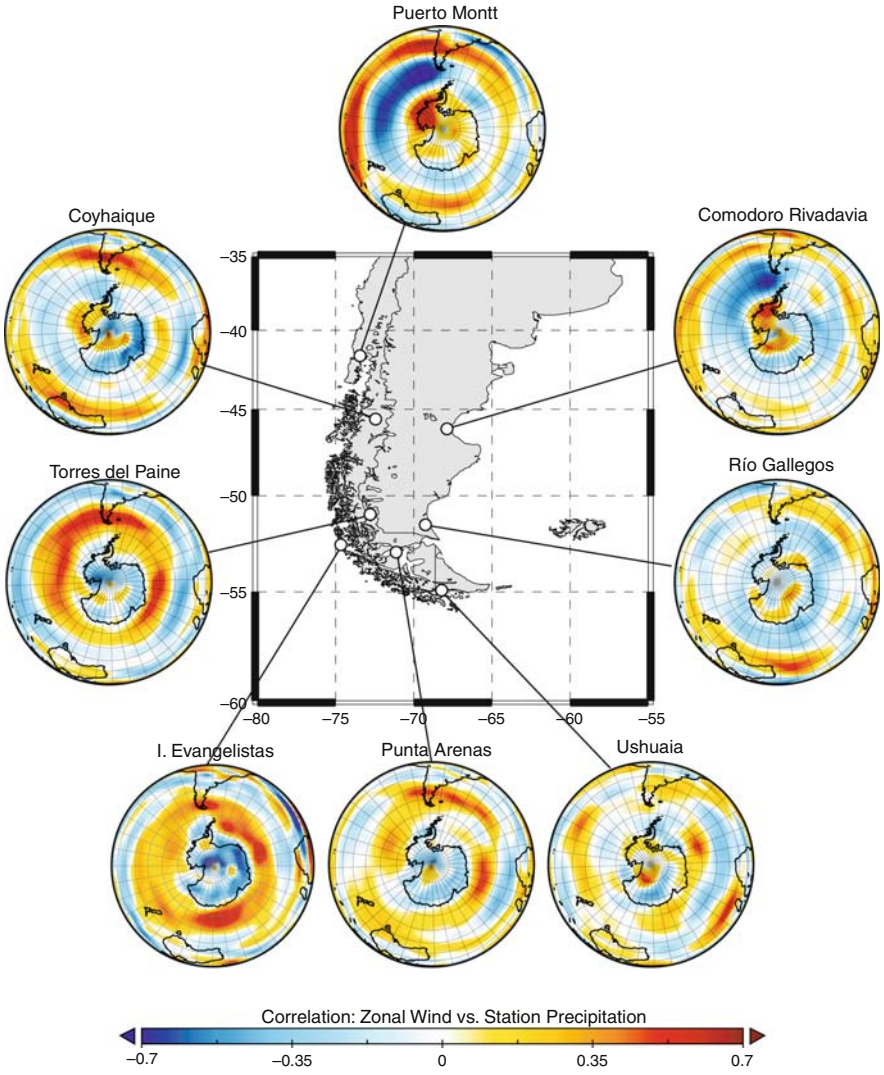

Fig. 15.3 Annual correlation between NCEP-NCAR reanalysis 700 hPa zonal wind in the Southern Hemisphere and selected precipitation records from Patagonia and Tierra del Fuego for the years 1983–2003 (Table 15.1). Meteorological stations proximal to the Andean divide exhibit positive correlations with atmospheric circulation, whereas locations closer to the Atlantic coast exhibit weak or negative correlations with the wind field. Color bar at base of map refers to correlation value (r value)

the wind field and a slight reduction in precipitation in western Patagonia. Northern Patagonia exhibits an overall reduction in summer precipitation and warmer surface air temperatures. The Pacific-South American (PSA) pattern of circulation is responsible for these observations largely through a wave train that extends from the western tropical Pacific to the mid to high southern latitudes (Mo 2000). Of

Table 15.1 Location and sources of monthly precipitation data obtained from meteorological stations in southern South America (see Fig. 15.1). The station data were used to evaluate the relationship between zonal wind and precipitation at annual timescales throughout Patagonia (Fig. 15.3) for the period 1983 to 2003

No.	Name	Latitude	Longitude	Elevation (m)	Source
1	Puerto Montt	−41.40	−73.10	81	Dirección Meteorológica de Chile
2	Coyhaique	−45.60	−72.10	311	Dirección Meteorológica de Chile
3	Commodoro Rivadavia	−45.80	−67.50	46	NOAA GHCN
4	Torres del Paine	−51.18	−72.97	25	Direccion General de Aguas
5	Río Gallegos	−51.60	−69.30	19	NOAA GHCN
6	Islote Evangelistas	−52.39	−75.10	52	Servicio Hidrográfico de la Armada de Chile (SHOA)
7	Punta Arenas	−53.00	−70.90	97	Dirección Meteorológica de Chile
8	Ushuaia	−54.80	−68.30	14	NOAA GHCN

particular relevance is the frequent occurrence of long-lived, tropospheric deep anticyclonic anomalies east of the southern tip of South America (centered at 50°S, 100°W) during El Niño years. These so-called blocking anticyclones at high latitudes are responsible for an equatorward migration of the storm track thus reducing precipitation over Patagonia.

Schneider and Geis (2004) and Fogt and Bromwich (2006) observe a non-stationary ENSO teleconnection with the high southern latitudes over decadal timescales. Specifically, relatively low correlations between meteorological variables and the southern oscillation index (SOI) during the 1980s increased after 1990. Using reanalysis data in a domain over the Southern Ocean, Fogt and Bromwich (2006) note that the Southern Annular Mode (SAM) plays an important role in modulating the strength of the ENSO signal in Western Antarctica and over the Pacific sector of the Southern Ocean: the ENSO teleconnection was particularly strong during periods when the SAM and the SOI index were positively correlated.

15.2.5 Southern Annular Mode (SAM)/Antarctic Oscillation (AAO) Variability

The Southern Annular Mode (SAM) or the Antarctic Oscillation (AAO) is the leading mode of atmospheric circulation in the high southern latitudes and plays a significant role in altering climate on seasonal and interannual timescales (Thompson

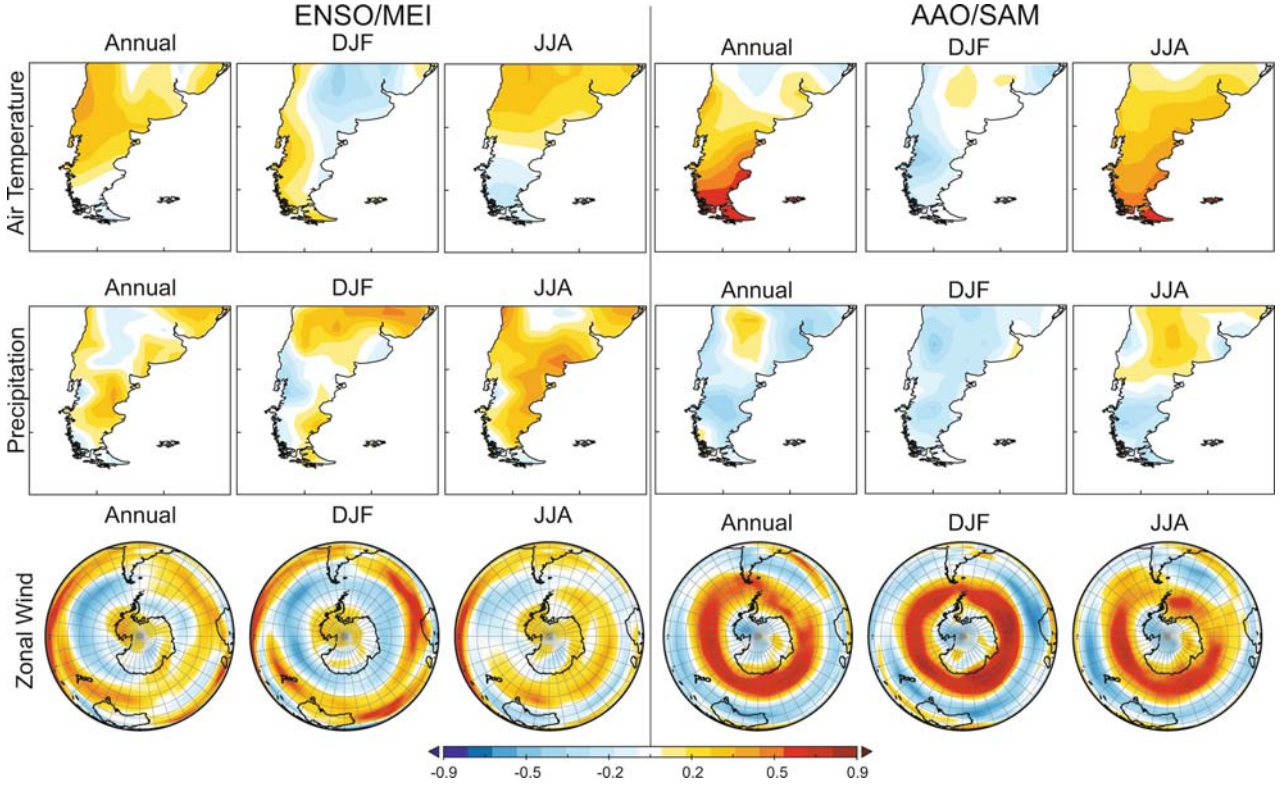

Fig. 15.4 Annual and seasonal correlations between NCEP surface air temperature, enhanced CMAP precipitation (Xie and Arkin 1997) and NCEP 700 hPa zonal wind (Kalnay et al. 1996) with indices of tropical (Multivariate ENSO Index) and high latitude (Southern Annular Mode) climate variability (1980–2006). Among the correlations presented here, most significant is the positive correlation between the SAM and the 700 hPa winds over the Southern Ocean and surface air temperature over southernmost South America. Most significant with respect to ENSO, are the negative correlations between the multivariate ENSO index (MEI) and the strength of the westerlies over the Pacific sector of the Southern Ocean and precipitation in western Patagonia during summer months (DJF)

and Wallace 2000). The SAM has been identified in both reanalysis and instrumental data, and the index is commonly defined as the leading empirical orthogonal function (EOF) of the 700 hPa geopotential height anomalies poleward of 20°S. The positive phase of the SAM is characterized by positive anomalies in atmospheric pressure over the mid-latitudes, negative pressure anomalies over Antarctica, and a strengthening of the atmospheric flow over the Southern Ocean across all longitudes (Marshall 2003). Figure 15.4 shows seasonal and annual spatial correlations of the SAM with zonal wind (NCEP), precipitation (CMAP) and air temperature (NCEP) from 1980 to 2006. Coincident with the positive phase of the SAM and relevant for interpreting paleoclimate archives from southern South America is an intensification and poleward shift of the westerlies, positive air temperature anomalies that increase with latitude, and a reduction in precipitation, particularly in northern Patagonia. Kwok and Comiso (2002) note that during the last two decades there has been a greater tendency towards the positive phase of the SAM and the negative phase of the Southern Oscillation. The Authors argue that the warming of air temperatures around the Antarctic Peninsula, adjacent ocean, and southernmost South America is a response due to the combined response of ENSO and the SAM. Although the SAM appears to be an important modulator of climate in southern South America, a number of questions remain concerning the origin or processes responsible for its long-term variability and trends. The recent increasing trend in the SAM, for example, has been attributed to such things as reductions in stratospheric ozone concentrations over the Antarctic continent (Thompson and Solomon 2002), increases in atmospheric CO_2 (Marshall 2003), and natural climate variability (Jones and Widmann 2004).

In summary, the meridional lay-out of southern South America allows the reconstruction of past variations in the strongly zonal westerly wind field. In many locations proximal to the Andes, zonal flow is positively correlated with precipitation. As a result of seasonal shifts in the latitudinal position of the westerlies, these correlations are seasonally dependent, with stronger correlations occurring during the summer in southern Patagonia and during the winter in northern Patagonia. Some of the stations east of the Andean divide (Torres del Paine and Coyhaique) show high variability in annual precipitation that is consistent with stations to the west of the Andean divide (I. Evangelistas). Farther to the east on the Atlantic coast and in central Argentine Patagonia, precipitation increases during periods of reduced westerly flow. Interannual climate variability in Patagonia is controlled, in part, by teleconnections with the tropics related to ENSO and variations in the SAM. These teleconnections manifest as anomalies in low-level wind strength, surface air temperature and precipitation. The strongest teleconnection in southern South America appears to be related to the SAM, where increasing surface air temperatures and poleward shifted westerlies coincide with the positive phase of the index.

15.3 Lake Sediment Records

15.3.1 Lago Guanaco

Moy et al. (2009) and Moreno et al. (2009) combined stable isotope and pollen data from Lago Guanaco, a small lake located in Torres del Paine National Park (51°S), to investigate past variations in atmospheric circulation (Fig. 15.1). The lake is located in the core of the modern wind field and precipitation falling in the region is well-correlated to the strength of the westerlies (Fig. 15.3). In addition, Lago Guanaco is an alkaline lake that preserves biogenic carbonate (bivalves, ostracodes, and *Chara* calcite) and it is situated close to the precipitation-controlled forest-steppe ecotone in southwest Patagonia. Two factors make Lago Guanaco an important site for reconstructing past changes in the westerlies. First, a strong positive correlation exists between precipitation and the strength of the westerly winds; increases in annual and seasonal precipitation correspond with increases in zonal wind speed across the Southern Hemisphere (Fig. 15.3). Second, two independent methods are available to evaluate changes in hydrology related to the westerlies. The first relies on reconstructing past changes in moisture balance by analyzing the oxygen isotopic composition ($\delta^{18}O$) of biogenic carbonates recovered from sediment cores. The second method utilizes a paleovegetation index that monitors zonal migrations of the boundary between the *Nothofagus* forests to the west and the Poaceae-dominated steppe to the east. Because this ecotone is controlled by moisture availability, increases in precipitation expand the forest to the east at the expense of the steppe.

Moy et al. (2008) collected a series of undisturbed sediment-water interface cores from Lago Guanaco and picked *Pisidium* sp. bivalves and extracted fine-fraction carbonate (<63 μm) from the sediment. The $\delta^{18}O$ of these two carbonate phases are shown in Fig. 15.5. Freshwater bivalves have been shown to precipitate their shell carbonate at or very close (within 1‰) to oxygen isotopic equilibrium (Dettman et al. 1999, Moreno et al. 2009, von Grafenstein et al. 1999), while the fine-fraction carbonate is likely derived from *Chara* growing in the littoral regions of the lake

Fig. 15.5 Compilation of paleoclimate proxies derived from Lago Guanaco (paleovegetation index and biogenic carbonate $\delta^{18}O$) and Siple Dome, Antarcica (Na^+). Concomitant increases in *Pisidium* $\delta^{18}O$ (**C**) and the *Nothofagus*/Poaceae ratio (**A**) are indicative of increased wind, enhanced evaporative conditions, and increased precipitation during the last 500 years and provide evidence for an enhancement of Southern Hemisphere circulation during the LIA. High $\delta^{18}O$ values and reduced paleovegetation index values centered at 800 cal year BP reflect increases in aridity coincident with the MCA. The variations observed in the Guanaco record show a strong similarity to the first EOF of Na+ concentration from Siple Dome, Antarctica (Kreutz et al. 1997) calculated using a 25- (*solid line*) and 115-year (*dashed line*) window (**B**). The vertical dashed line is the calculated break in slope that Kreutz et al. (1997) use to identify the start of the LIA, the red rectangle corresponds to drought termination in central Patagonia inferred from radiocarbon-dated trees exposed in Patagonia lakes (Stine 1994), and the triangles at the base of the plot refer to median calibrated ages used in the Lago Guanaco age model. The paleovegetation index declines at ~150 cal year BP due to widespread clearance of the Nothofagus forest for livestock grazing

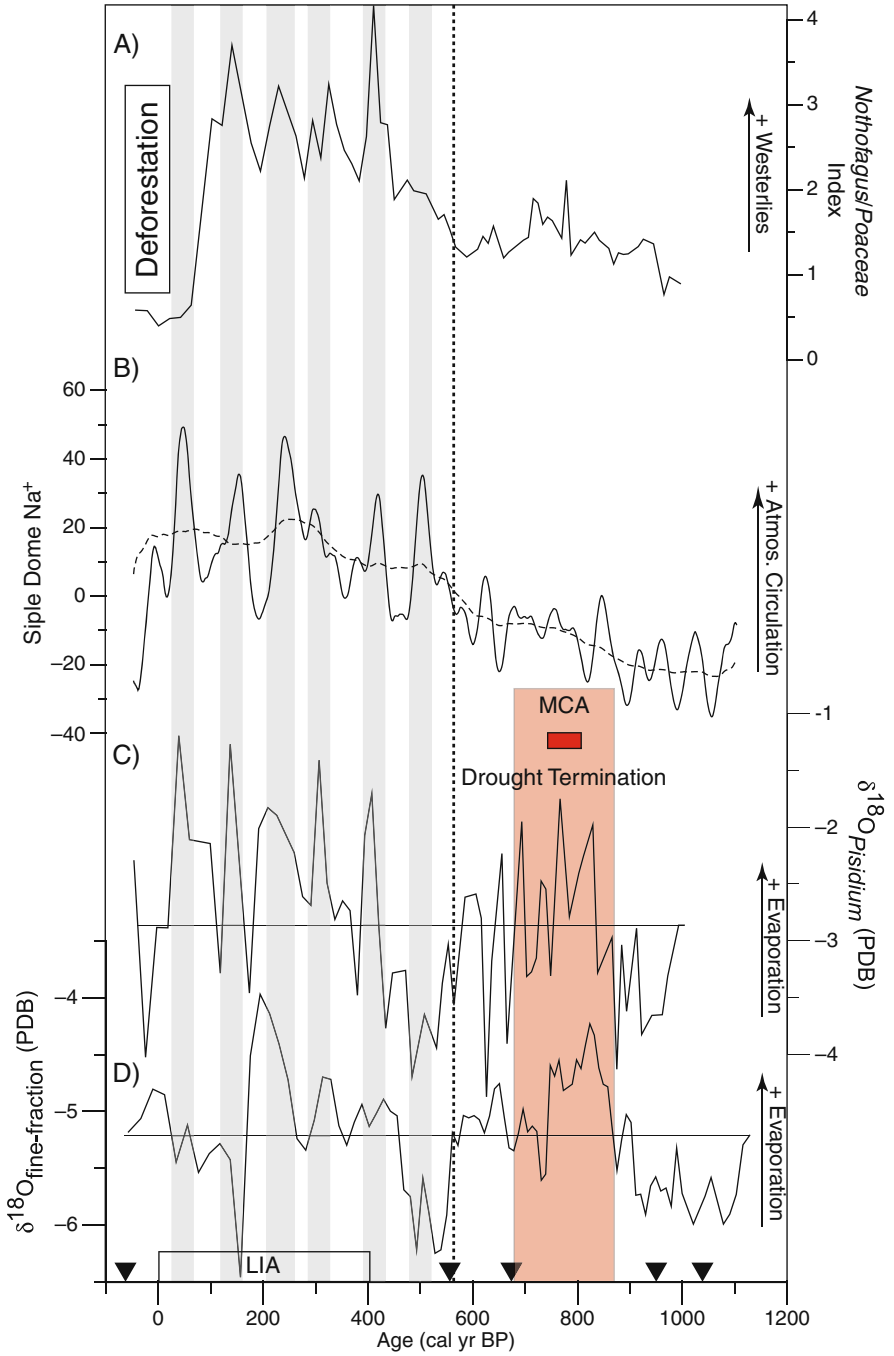

Fig. 15.5 (continued)

and is offset from equilibrium values by >2‰ (Moy et al. 2008). Despite these differences, however, we generally see similar variations in both isotope stratigraphies during the last 1200 years over centennial timescales (Fig. 15.5). Minor divergences between the two isotopic profiles, especially on shorter timescales such as during the last 200 years, may be related to seasonal changes in fine-fraction calcification.

The annual weighted average of the isotopic composition of precipitation entering the lake is ~–10.5‰ based on data from IAEA/WMO stations in Punta Arenas and Coyhaique, and the average isotopic composition of groundwater measured from a nearby well in January 2007 was –13.9‰. In contrast to these hydrologic inputs, the measured $\delta^{18}O$ of the lake water during January 2007 was –4.05‰ VSMOW and average core-top $\delta^{18}O$ value for PS0711SC is –3.7‰ VPDB. The > 6‰ discrepancy indicates a significant isotopic enrichment of $\delta^{18}O$ due to evaporative effects. Today, the lake level is ~1.5 m below a spillway that drains water to Lago Sarmiento and is hydrologically closed. Evaporation is the major mechanism for water loss, and evaporative processes dominate the $\delta^{18}O$ signal in the *Pisidium* and fine-fraction carbonate (Leng and Marshall 2004, Moy et al. 2008).

We compile the oxygen isotopic data from *Pisidium* and the fine-fraction carbonate (Moy et al. (2008); Fig. 15.5) to illustrate changes in hydrologic balance in the last millennium. The two profiles exhibit similar variability over the last 1200 years, and the Authors identify two periods of above-average $\delta^{18}O$ values between 900 and 600 cal year BP and between 400 and 0 cal year BP. Centered on 1100 and 500 cal year BP are two century-long intervals of below average $\delta^{18}O$. The periods of above-average $\delta^{18}O$ are indicative of increased evaporative processes coincident with the MCA and the LIA.

Moreno et al. (2009) calculated a paleovegetation index based on the ratio of *Nothofagus*/Poaceae pollen to identify changes in the relative abundance of forest and steppe. Positive anomalies indicate dominance of *Nothofagus* forests and negative anomalies indicate steppe. During the last two millennia, increases in the paleovegetation index occurred at 1300 and 570 cal year BP. High positive anomalies between 570 and 100 cal year BP are interpreted as an eastward expansion of the *Nothofagus* forest during LIA due to increased precipitation and westerly atmospheric flow (Fig. 15.5). The large decrease in the last 100 years is attributed to forest clearance by European settlers and is coincident with high charcoal concentrations and of the presence of the introduced herb *Rumex acetosella*.

Combining the paleovegetation index and the oxygen isotope data from the two carbonate fractions provides new insight into past variations in the westerlies. During the MCA, above-average $\delta^{18}O$ values indicating aridity are associated with relatively dry centennial-scale phases inferred from the paleovegetation index. Peak isotopic values at Lago Guanaco that span 200 years and are centered on ~800 cal year BP, coincide with the age of submerged tree stumps from two Patagonian lakes that have been interpreted to indicate drought termination during and after the MCA (Stine 1994).

During LIA time, a significant and complex change takes place in the relationship between the $\delta^{18}O$ and the paleovegetation index. Moy et al. (2008) observe

an increase in both parameters that is interpreted as an increase in the strength of the westerlies at this latitude. The reasoning is that increased wind stress on the lake would increase isotopic fractionation through evaporative effects. At the same time, stronger westerlies would also increase precipitation and promote forest expansion, increasing the paleovegetation index. At multi-decadal timescales, consistent variations in the *Pisidium* $\delta^{18}O$ values and paleovegetation index may reflect the enhanced delivery of *Nothofagus* pollen to the coring site during periods of increased westerly wind speeds. The paleovegetation index are highest during the LIA than any other time in the last 5000 years suggesting that westerly wind strength culminated during this time (Moreno et al. 2009).

Moy et al. (2008) compared the results from Lago Guanaco with the record of Na^+ from the Siple Dome ice core in western Antarctica, which reflects enhanced atmospheric circulation and delivery of sea salt derived Na^+ to the coring site (Kreutz et al. 1997). To identify important multi-decadal and longer variations in this time series, the first EOF with 25- and 115-year windows were calculated using singular spectrum analysis (SSA) (Ghil et al. 2002) (Fig. 15.5). The Na^+ time series in Siple Dome exhibits significant multi-decadal variability between 550 and 0 cal year BP that is superimposed upon a long-term trend of increasing values. The increase in Na^+ coincides with the prominent increase in the paleovegetation index, and high values in *Pisidium* $\delta^{18}O$ data at L. Guanaco, all three records exhibit sustained high values until ~150 cal year BP, when the pollen index values decline due to widespread forest clearance. Although the Guanaco *Pisidium* $\delta^{18}O$ and the Siple Dome record (25-year window) show consistent in-phase multi-decadal variations during the LIA, the inherent uncertainty in the calibrated radiocarbon chronology precludes a close evaluation of this relationship.

In summary, we highlight two important findings regarding climate change in southern Patagonia during the last millennium. A period of aridity (reduced westerlies) coincides with the timing of the MCA and an extended period of increased evaporation and precipitation occurs during the LIA. The former interval reflects periods of aridity in the region, whereas the latter indicates an overall increase in the strength of atmospheric circulation in the high southern latitudes.

15.3.2 Laguna Potrok Aike

Directly to the east of Lago Guanaco in Argentine Patagonia, a number of paleoclimate archives have been derived within the project SALSA (South Argentinean Lake Sediment Archives and modeling). Sediment sequences have been recovered from lakes within the Pali Aike volcanic field, including Laguna Potrok Aike (Haberzettl et al. 2007, Haberzettl et al. 2005, Mayr et al. 2007, Wille et al. 2007), Laguna Azul (Mayr et al. 2005), and from the tarn Laguna de las Vizcachas on the Meseta de las Vizcachas (Fey et al. In Press). Based on seismic stratigraphy, Laguna Potrok Aike has a ~300-m-thick sediment sequence (Anselmetti et al. 2009). Because the lake is located beyond the late-Quaternary ice limit, Laguna Potrok Aike has the potential to provide a long record (i.e. multiple glacial cycles)

of climate change in Southern Patagonia and has been drilled by the International Continental Scientific Drilling Program (ICDP) in late 2008.

Haberzettl et al. (2005, 2008) combined geochemical, palynological, and physical property data from sediment cores collected in the 100-m-deep central basin and in the littoral zone of Laguna Potrok Aike and inferred changes in lake level during the last ~2000 years. By combining the different proxies, namely wt.% total inorganic carbon, Ti, C/N, and $\delta^{13}C$, the Authors highlight a period of lowered lake levels between 720 and 470 cal year BP and a period of increased lake levels and relatively moist conditions between ~450 and 0 cal year BP. The former period is attributed to aridity during the MCA, while the latter is related to relatively wet conditions during the LIA. Similarly, in Laguna Azul, Mayr et al. (2005) identify a sequence of hydrologic changes between 550 and 250 cal year BP (dry) and 250 and 50 cal year BP (wet) also using a multi-proxy approach but focusing on the $\delta^{13}C$ of bulk organic matter. Both studies suggest that changes in the strength of the southern westerlies during the last two millennia caused the lake-level variations. Although the late Holocene wet and dry periods interpreted from Laguna Potrok Aike and Laguna Azul generally mirror results from Lago Guanaco, the modern relationship between wind and precipitation indicates that intervals of enhanced westerly intensity should produce wetter conditions in western Patagonia and drier conditions in the east (Mayr et al. 2007, Moy et al. 2008). Therefore, westerly-driven wet/dry cycles should be antiphased between the L. Potrok Aike/L. Azul and Lago Guanaco records. Yet geochemical proxies from these three lakes suggest that both east and west Patagonia were wet during the LIA and dry during the MCA, yielding opposite interpretations of westerly wind behavior. This discrepancy will best be reconciled by the establishment of additional weather stations in southern Patagonia and by the development of additional paleoclimate reconstructions from the Patagonian interior.

15.3.3 Lago Cardiel

Past climate change and related lake level variations have also been reconstructed at Lago Cardiel (49°S; Fig. 15.1), located in central Patagonia and on the eastern Andean slope. Lago Cardiel is a large closed-basin lake with a modern surface area of 370 km^2 and a maximum water depth of 76 m (Markgraf et al. 2003). Galloway et al. (1988) and Stine and Stine (1990) reconstructed former lake high stands by radiocarbon dating both sediments and tufas exposed in stream cuts and strandlines encircling the modern lake. An impressive shoreline transgression was centered at ~10500 cal year BP, when the lake surface was > 50 m above the 1990 lake level. During the late Holocene, Stine and Stine (1990) document smaller (< 10 m) variations in lake level and identify 4 transgressions during the last 2000 years centered at ~2000, ~1200, ~800 and ~200 cal year BP. The 1990 lake level is considered a relatively low elevation for the Holocene and the culmination of a regression that began ca. AD 1940 (Markgraf et al. 2003). Recently, the lake has risen at least 4 m since this 1990 position, possibly as a result of ENSO-induced precipitation (Markgraf et al. 2003).

Gilli et al. (2001 and 2005) compared seismic surveys of the sediment stratigraphy and the physical properties from a number of cores from Lago Cardiel to identify variations in climate during the Holocene, and Markgraf et al. (2003) presented geochemical and paleoenvironmental (diatoms and pollen) data collected from multiple coring sites within the lake. These studies characterize the last 2000 years of climate history as highly variable with alternating wet and dry periods, possibly related to the increase in ENSO variability. The Holocene chronology is derived from two tephra found in the sediment cores: the older tephra is derived from Volcán Hudson at ~7500 cal year BP (Naranjo and Stern 1998) and the younger is from the Northern Austral Volcanic Zone (NAVZ) at ~3200 cal year BP (Markgraf et al. 2003). Radiocarbon dates on carbonate and organic fractions preserved in the sediment cores provide a range of ages that are older than the tephrochronology by >3000 years (Gilli et al. 2005). The offset has been attributed to two processes: a variable reservoir effect that is dependent on lake volume and contamination from the erosion of older sediment within the watershed. Unfortunately, the two ages that constrain the Holocene tephrochronology make it difficult to compare results with other paleoclimate records.

15.4 Pollen and Charcoal Records

Pollen records derived from lakes and bogs represent one of the most abundant paleoclimate archives in southern South America. Since the pioneering work by Auer (1933, 1958), many studies have reconstructed the ecological and climatic history over a range of time periods (Heusser 1966, Heusser and Heusser 2006, Heusser et al. 1999, Markgraf 1993, Markgraf et al. 2003, Moreno 2004, Moreno et al. 1999, Villagrán 1985, 1988). However, few palynological records in Patagonia have adequate chronology and sampling resolution to address environmental changes of the past 2000 years. Two records from small closed-basin sites located in the rainforest-dominated region of the Chilean channels and the Andean region of Central Patagonia (~45°S) (Szeicz et al. 2003, 1998) are exceptional because they link changes in vegetation changes and fire regimes (inferred from the presence of charcoal particles in the sediments) on decadal timescales over the last millennium. These records indicate little or no variation in the vegetation and fire regime since ~1900 cal year BP, with the exception of a decline in forest dominance associated with European settlement and forest clearance by ~1890 AD.

Pollen records from southern Patagonia (50–52°S) show a varied response to climate change during the last 2000 years. High-resolution pollen and plant macrofossil records from the Río Rubens bog (Huber and Markgraf 2003), located in the deciduous forest zone of Southern Patagonia (51.5°S) east of the Andes, indicate the presence of *Nothofagus* forests (probably *N. pumilio*) with little or no variations in vegetation since ~5000 cal year BP. Intense fires at ~350 cal year BP led to the expansion of grasslands with exotic species of European origin (*Rumex acetosella*). Likewise, a pollen record from Lago Potrok Aike (Haberzettl et al. 2005), directly east in the Patagonian steppe, shows dominance of steppe herbs and shrubs over the last ~1900 years and the expansion of *Rumex acetosella* at ~1850 AD. The

pollen record from Lago Guanaco (Fig. 15.5) shows a pulse of forest expansion starting at 1300 cal year BP and increasing between 570 and 70 cal year BP. The data are interpreted as evidence of an eastward shift of the forest-steppe ecotone and an intensification and/or latitudinal shift of the westerly winds (see previous discussion). The fact that L. Potrok Aike, Rio Rubens bog, and Lago Guanaco lie within 200 km of each other, but show different signals, can be attributed to the location of the records in different ecological environments (i.e. steppe vs. forest), the depositional environment (lake vs. bog), chronologic control, and local differences in the sensitivity of the forest-steppe ecotone to changes in precipitation (Moreno et al. 2009). In addition, a complicating factor for the interpretation of pollen records from Patagonia is that the palynomorph *Nothofagus dombeyi*-type includes species found in a broad range of habitats and climatic regimes (*N. antarctica, N. betuloides, N. dombeyi, N. nitida, N. pumilio*), including azonal habitats such as wetlands. By dwelling on the surface or the periphery of fens and bogs, species such as *Nothofagus antarctica* can impose a biased palynological signal in the sedimentary record that overrides the extralocal or regional one. Future regional-scale interpretations of past vegetation and climate change in Patagonia should take these issues into account.

The occurrence of natural fires depends on the accumulation, quality, and spatial/temporal continuity of biomass, their desiccation, and ignition sources. The stratigraphic analysis of charcoal particles allows reconstruction of past fire regimes, and thus allows inferences to be drawn about past variability in hydrologic balance, seasonality, and ignition sources at multiple scales of analysis. Charcoal records from the rainforest region of NW Patagonia (∼41°S) indicate the culmination of a multi-millennial increase in fire activity that started at ∼3000 cal year BP (Whitlock et al. 2007) and peaked ∼1100 years ago. Macroscopic charcoal records from two closed-basin lakes (Pichilaguna and El Salto) in the Longitudinal Valley of the Chilean Lake District indicate centennial-scale variations (Fig. 15.6), including periods of high charcoal abundance between ∼1200–1000 and 500–250 cal year BP, and low values between 900–500 and 250–0 cal year BP. A palynological site from Isla Grande de Chiloé shows changes in forest composition that suggests high levels of disturbance in the last 500 years (Abarzua and Moreno 2008). This increase was followed by high levels of charcoal from recent European-set burning. The climatic significance of the latter remains unclear as the disturbance signal in the vegetation overrides or obscures a genuine climatic response. A high-resolution study of a 600-year old sedimentary record from Lago Puyehue by Bertrand et al. (2005) revealed a distinctive peak in terrigenous supply between 450 and 250 cal year BP, which was interpreted as a prominent wet phase followed by a steady decline toward the present. This putative wet phase was contemporaneous with intense fire activity in Pichilaguna and El Salto, thus suggesting that fire activity in the Longitudinal Valley of the Lake District between 500 and 250 cal year BP was caused by humans, or mechanisms other than increased precipitation can account for increased terrigenous supply to Lago Puyehue. Additional high-resolution precisely dated paleoclimate records from this area are needed to solve this apparent mismatch.

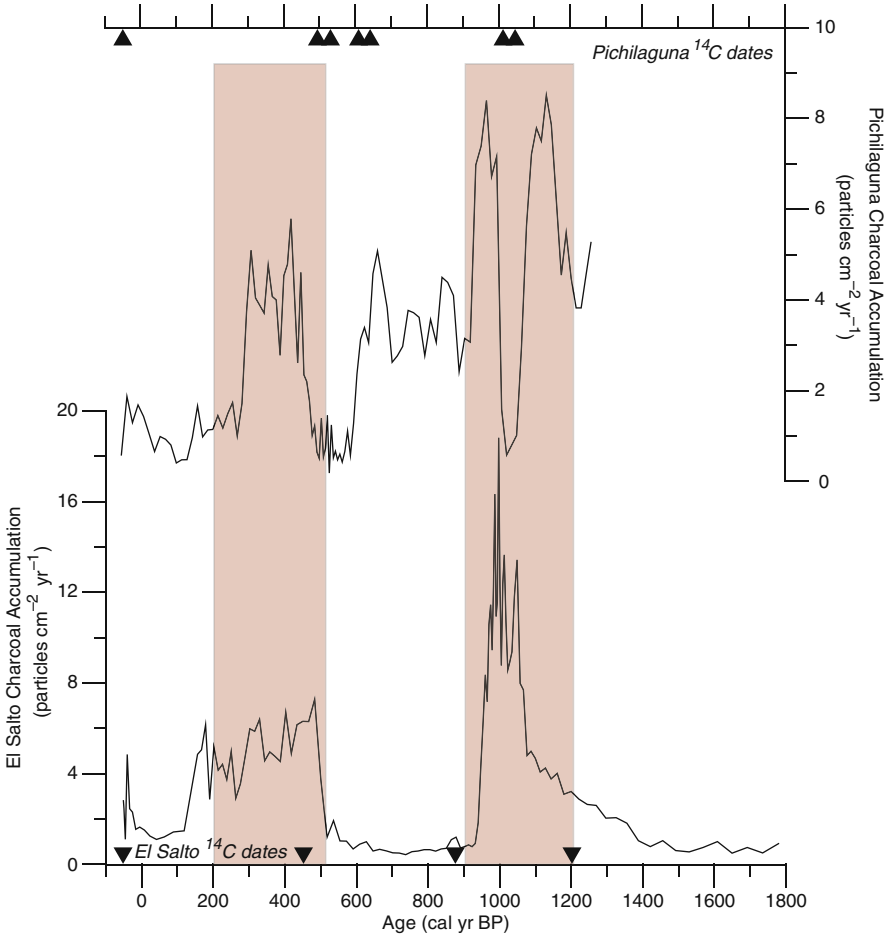

Fig. 15.6 Charcoal accumulation rates from Pichilaguna and El Salto highlight the last ~1200 cal year BP of fire history in the Chilean Lake District (42°S). These two records display alternating periods of high charcoal abundance between ~1200–1000 and 500–200 cal year BP (vertical red bars), and intervals with relatively low values between 900–500 and 200–0 cal year BP. Black triangles refer to median calibrated radiocarbon ages used in the chronology

15.5 Glacier Records

The Campo de Hielo Patagónico Norte (CHPN) and Sur (CHPS) are the most prominent glacial features in southern South America, and when combined, they represent the largest and most extensive areas of ice in the Southern Hemisphere outside Antarctica (Casassa et al. 1998). The northern and southern ice fields have aerial extents of ~4200 and ~13000 km^2, respectively (Rignot et al. 2003). The CHPN has average elevations between 1000 and 1500 m from west to east and the CHPS has average elevations of 1500 to 2000 m (Aniya 1988, Aniya et al. 1996, Rivera et al. 2007, Warren and Sugden 1993). Both ice fields have exten-

sive outlet glaciers that terminate in the Chilean fjords, into freshwater lakes, or on land (Casassa et al. 2002). The Southern Hemisphere westerlies transport massive amounts of precipitation to both ice sheets (present-day accumulation rates of up to 10 m water equivalent per year), but the eastern outlet glaciers terminate in areas that receive a fraction of the amount received in the west or at the divide (Rivera et al. 2007). Because of the difficulty of field work and obtaining clear satellite imagery in this very wet region, the high-elevation ice fields remain relatively poorly studied.

20th century research indicates that climate *in general* has been the dominant driver of glacial changes but the nature of the terminal environment, and other "non-climate effects" are important second-order controls for particular glaciers (Harrison et al. 2007, Naruse 2006, Rignot et al. 2003, Warren and Sugden 1993). Patagonian glaciers are sensitive climate proxies that respond to temperature (<0.5°C) and precipitation, with the former being relatively most important for most glaciers in the latter part of the 1900s (Rignot et al. 2003, Rivera and Casassa 2004). Many outlet glaciers radiating from the ice fields have been retreating from their LIA maximum positions since the late 19th century, (Harrison et al. 2007). Recent work has focused on quantifying the rate of ice-volume loss, which has increased relatively rapidly towards the present and are considered large enough to account for ~6% of recent global sea level rise (Rignot et al. 2003).

Clapperton and Sugden (1988), Porter (2000), and Glasser et al. (2004) reviewed the history of glacial ice activity in southern South America in the mid and late Holocene. Given the remoteness of glaciers in Patagonia, only a few areas have been investigated in detail. Paleoclimate knowledge is based largely on the research of Mercer (1965, 1968, 1970, 1976, 1982), Porter (2000), Röthlisberger (1986), Malagnino and Strelin (1992), Aniya (1995), Aniya et al. (1996), Strelin and Malagnino (2000), and Harrison et al. (2007). Most of the data for glacial ice expansion is derived from radiocarbon-dated glacial deposits on outlet and satellite glaciers in the northern and southern Patagonian ice fields. In addition to radiocarbon chronologies, lichenometry (Harrison et al. 2008) and tree-ring derived chronologies (Harrison et al. 2007, Koch and Killian 2005, Villalba 1994) have been used to date recent (last millennium) moraine deposits. Cosmogenic surface-exposure ages have been used to date middle Holocene and older deposits in southern South America (Douglass et al. 2005).

Porter (2000) highlighted some of the challenges that must be considered when interpreting and identifying the timing of past glacial ice extents. Radiocarbon age-dating of glacial deposits can be challenging due to the difficulty of finding suitable or relevant organic material. Minimum or maximum limiting ages may not closely constrain the timing of ice advance, and organic material may be remobilized or contaminated by younger material. Also, many studies rely on single minimum or maximum age limits for the timing of a glacial advance. Modern process studies show, internal ice instabilities due to changes in the calving environments in lakes and fjords, in addition to rockfall deposits on glacier ablation areas, are secondary mechanisms that should also be considered when interpreting past changes in ice extent (Porter 2000). In addition to these local or site-specific challenges, whether temperature or precipitation is the primary climate mechanism driving past changes in ice extent has been questioned. Glasser et al. (2002) suggested that outlet

glaciers on the eastern side of the Andes may be particularly sensitive to changes in precipitation, largely due to the steep rainfall gradient that exists from west to east across the topographic divide. However, eastern outlet glaciers, from the ice fields at least, are also ultimately nourished by the high ice accumulation areas on the divide and ablation areas on the eastern side still occur in areas classified as much wetter than semi-arid (e.g., see weather data listed above for Torres del Paine). In addition, because the westerlies are driven by atmospheric and oceanic temperature gradients, increases in accumulation in the past may have been coupled with reductions in temperature (see above), facilitating ice expansion. Nonetheless, glacial response and its relative magnitude to a climatic change may vary across the Andean divide, and evidence from multiple sites (and with multiple chronostratigraphies) is needed to provide a robust chronology of glacial response to climate change (Porter 2000).

Evidence from radiocarbon-dated deposits from outlet and satellite glaciers from the northern and southern Patagonian ice fields indicates that Neoglaciation in southern South America began, and was most extensive, in the mid Holocene ca. ~5400 cal year BP (e.g., Mercer 1976). Mercer described advances from his work in the Patagonian ice fields at ~4600 cal year BP, ~2500 cal year BP, and during the last few hundred years. The Mercer chronology was replaced with the four event Clapperton and Sugden (1988) and Aniya (1995) model, which had glacial maxima at ~3800 cal year BP, ~2700–1900 cal year BP, ~1400–1200 cal year BP, and the last few hundred years (also see Porter 2000).

We compiled radiocarbon and tree-ring evidence for glacial advances during the last 2000 years in Patagonia (In Fig. 15.7 and Table 15.2). We calibrated the radiocarbon ages using the Southern Hemisphere calibration curve (McCormac et al. 2004) and present the results in calendar year BP to facilitate comparison with other paleoclimate records presented in this review. Many of the ages presented here reflect a minimum age of ice advance (i.e., the radiocarbon dates were either derived from peat that started growing after the ice retreated or from deposits on top of the moraine). When the ages are combined, we identify three periods of increased glacial ice extent in Patagonia and Tierra del Fuego during the last 2000 years centered on 1300 cal year BP, 600 cal year BP, and between 400 and 50 cal year BP (Fig. 15.7).

15.6 Tree-Ring Records

Tree-ring records from southern South America represent the most broadly distributed and annually resolved paleoclimate archives. Tree-ring networks derived from sensitive locations can be used to reconstruct large-scale atmospheric circulation patterns at annual to multi-decadal timescales (Aravena et al. 2002, Lara et al. 2001, Lara and Villalba 1993, Lara et al. 2008, Villalba 1990, 1991, 1994). Records from southernmost South America, for example, are well-poised to reconstruct climate variability related to the SAM and therefore can significantly expand our understanding of the potential magnitude of change and timescales of variability (Villalba 2007).

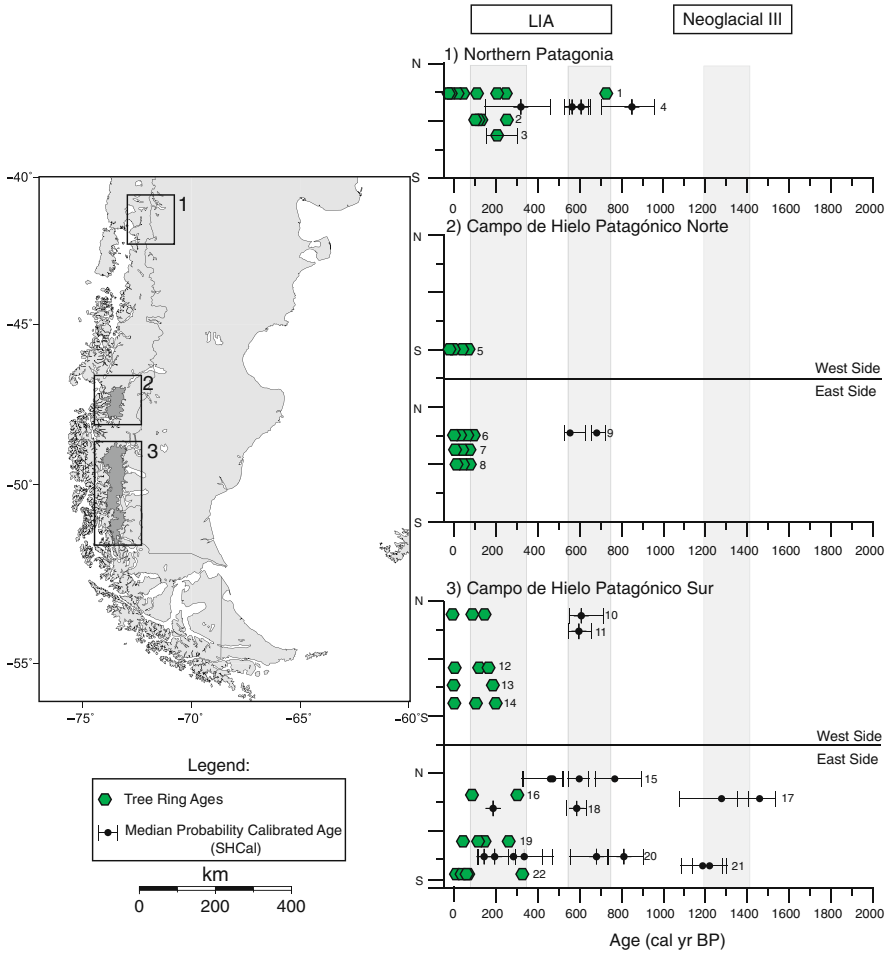

Fig. 15.7 Summary of glacial advances in southern South America during the last 2000 years. Glacial activity derived from tree rings and from radiocarbon dates on glacial deposits are shown for three regions. We calibrated the ages published in the literature using the Southern Hemisphere calibration curve (McCormac et al. 2004), show the median probability age along with the 1-sigma range, and plot the data on the calibrated age scale (cal year BP). See Table 15.2 for data sources, locations, and references for the dated glacial deposits. We highlight three periods of enhanced glacial activity (vertical bars): (1) between 1400 and 1200, (2) 550 and 750, and (3) 400 and 50 cal year BP. Ice generally began retreating from LIA ice positions in the late 19th century (Harrison et al. 2007, Villalba et al. 2005)

Villalba et al. (2003) compiled a network of tree-ring records derived from upper treeline locations in northern and southern Patagonia to investigate changes in temperature during the last four centuries (Fig. 15.8). These records were processed to highlight multi-decadal variations in mean annual temperature, and therefore, are especially useful for placing the modern temperature observations in a longer context that can be compared with paleoclimate records from these regions. In Fig. 15.8,

Table 15.2 Compilation of calibrated radiocarbon dates and tree ring ages for timing of glacial activity in southern South America. T, R, L refer to tree-ring, radiocarbon, and lichenometry age dating techniques, respectively and CHPN and CHPS refer to Campo de Hielo Patagónico Norte (CHPN) and Sur (CHPS)

Figure 7 References	Glacier name	Location	References	Latitude	Type	Median calibrated age (SHCal) or tree-ring age	1 sigma range for ^{14}C
1	Frías	Mt. Tronador	Villalba (1990)	−40.17	T	>714	–
1	Frías	Mt. Tronador	Villalba (1990)	−40.17	T	312	–
1	Frías	Mt. Tronador	Villalba (1990)	−40.17	T	228	–
1	Frías	Mt. Tronador	Villalba (1990)	−40.17	T	203	–
1	Frías	Mt. Tronador	Villalba (1990)	−40.17	T	111	–
1	Frías	Mt. Tronador	Villalba (1990)	−40.17	T	69	–
1	Frias	Mt. Tronador	Villalba (1990)	−40.17	T	36	–
1	Frías	Mt. Tronador	Villalba (1990)	−40.17	T	−2	–
1	Frías	Mt. Tronador	Villalba (1990)	−40.17	T	−27	–
1	Frías	Mt. Tronador	Villalba (1990)	−40.17	T	250	–
3	Río Manso	Mt. Tronador	Lawrence and Lawrence (1959)	−41.0	T	250	–
3	Río Manso	Mt. Tronador	Lawrence and Lawrence (1959)	−41.0	T	135	–
3	Rio Manso	Mt. Tronador	Lawrence and Lawrence (1959)	−41.0	T	117	–
3	Río Manso	Mt. Tronador	Lawrence and Lawrence (1959)	−41.0	T	103	–
4	Río Manso	Mt. Tronador	Rabassa et al. (1984)	−41.0	T,L,R	180−300	–
2	Río Manso	Mt. Tronador	Röthlisberger (1986)	−41.0	R	822	685−927
2	Río Manso	Mt. Tronador	Röthlisberger (1986)	−41.0	R	590	535−633
2	Río Manso	Mt. Tronador	Röthlisberger (1986)	−41.0	R	549	515−624
2	Río Manso	Mt. Tronador	Röthlisberger (1986)	−41.0	R	315	152−451
5	Gualas and Reicher	CHPN	Harrison and Winchester (1998)	−46.5	T	74	–
5	Gualas and Reicher	CHPN	Harrison and Winchester (1998)	−46.5	T	41	–
5	Gualas and Reicher	CHPN	Harrison and Winchester (1998)	−46.5	T	−4	–
5	Gualas and Reicher	CHPN	Harrison and Winchester (1998)	−46.5	T	−20	–
6	Soler	CHPN	Sweda (1987)	−47.0	T	100−90	–
6	Soler	CHPN	Sweda (1987)	−47.0	T	60−50	–

Table 15.2 (continued)

Figure 7 References	Glacier name	Location	References	Latitude	Type	Median calibrated age (SHCal) or tree-ring age	1 sigma range for ^{14}C
6	Soler	CHPN	Sweda (1987)	−47.0	T	40−30	–
6	Soler	CHPN	Sweda (1987)	−47.0	T	10−0	–
7	Arco, Arenales, and Colonia	CHPN	Harrison and Winchester (2000)	−47.25	T	75	–
7	Arco, Arenales, and Colonia	CHPN	Harrison and Winchester (2000)	−47.25	T	45	–
7	Arco, Arenales, and Colonia	CHPN	Harrison and Winchester (2000)	−47.25	T	5	–
8	Nef	CHPN	Winchester et al. (2001)	−47.2	T	87	–
8	Nef	CHPN	Winchester et al. (2001)	−47.2	T	66	–
8	Nef	CHPN	Winchester et al. (2001)	−47.2	T	15	–
9	Soler	CHPN	Glasser et al. (2002)	−47.0	R	553	525–625
9	Soler	CHPN	Glasser et al. (2002)	−47.0	R	680	660–720
10	Ofhidro Norte	CHPS	Mercer (1970)	−48.4	R	697	570–765
10	Ofhidro Norte	CHPS	Mercer (1970)	−48.4	T	95	–
10	Ofhidro Norte	CHPS	Mercer (1970)	−48.4	T	100	–
10	Ofhidro Norte	CHPS	Mercer (1970)	−48.4	T	155	–
11	Ventisquero Bravo	CHPS	Röthlisberger (1986)	−48.0	R	600	555–650
11	Ventisquero Bravo	CHPS	Röthlisberger (1986)	−48.0	R	Modern (< 200 cal year BP)	–
11	Ventisquero Bravo	CHPS	Röthlisberger (1986)	−48.0	R	Modern (< 200 cal year BP)	–
12	Bernardo	CHPS	Mercer (1970)	−48.6	T	175	–
12	Bernardo	CHPS	Mercer (1970)	−48.6	T	140–130	–
12	Bernardo	CHPS	Mercer (1970)	−48.6	T	10–0	–
13	Témpano	CHPS	Mercer (1970)	−48.65	T	200–180	–
13	Témpano	CHPS	Mercer (1970)	−48.65	T	10–0	–

Table 15.2 (continued)

Figure 7 References	Glacier name	Location	References	Latitude	Type	Median calibrated age (SHCal) or tree-ring age	1 sigma range for ^{14}C
14	Hammick	CHPS	Mercer (1970)	−48.8	T	200	–
14	Hammick	CHPS	Mercer (1970)	−48.8	T	110	–
14	Hammick	CHPS	Mercer (1970)	−48.8	T	10–0	–
15	Ventisquero Huemul	CHPS	Röthlisberger (1986)	−48.0	R	604	555–650
15	Ventisquero Huemul	CHPS	Röthlisberger (1986)	−48.0	R	202	145–310
15	Ventisquero Huemul	CHPS	Röthlisberger (1986)	−48.0	R	332	154–453
15	Ventisquero Huemul	CHPS	Röthlisberger (1986)	−48.0	R	446	332–501
15	Ventisquero Huemul	CHPS	Röthlisberger (1986)	−48.0	R	469	334–529
15	Ventisquero Huemul	CHPS	Röthlisberger (1986)	−48.0	R	480	341–527
15	Ventisquero Huemul	CHPS	Röthlisberger (1986)	−48.0	R	775	681–900
16	Narvarez	CHPS	Mercer (1968)	−48.0	T	300	–
16	Narvarez	CHPS	Mercer (1968)	−48.0	T	70	–
17	Upsala	CHPS	Aniya (1995)	50.0	R	1464	1358–1539
17	Upsala	CHPS	Aniya (1995)	50.0	R	1283	1083–1413
18	Ventisquero Frances	CHPS	Röthlisberger (1986)	−51.0	R	Modern (< 200 cal year BP)	–
18	Ventisquero Frances	CHPS	Röthlisberger (1986)	−51.0	R	606	559–649
19	Grey	CHPS	Marden and Clapperton (1995)	−51.5	T	290–225	–
19	Grey	CHPS	Marden and Clapperton (1995)	−51.5	T	145	–
19	Grey	CHPS	Marden and Clapperton (1995)	−51.5	T	105	–
19	Grey	CHPS	Marden and Clapperton (1995)	−51.5	T	< 60	–
20	Ventisquero Perro	CHPS	Röthlisberger (1986)	−51.0	R	Modern (< 200 cal year BP)	–
20	Ventisquero Perro	CHPS	Röthlisberger (1986)	−51.0	R	226	148–320
20	Ventisquero Perro	CHPS	Röthlisberger (1986)	−51.0	R	312	152–446
20	Ventisquero Perro	CHPS	Röthlisberger (1986)	−51.0	R	361	289–492

Table 15.2 (continued)

Figure 7 References	Glacier name	Location	References	Latitude	Type	Median calibrated age (SHCal) or tree-ring age	1 sigma range for ^{14}C
20	Ventisquero Perro	CHPS	Röthlisberger (1986)	−51.0	R	691	571–744
20	Ventisquero Perro	CHPS	Röthlisberger (1986)	−51.0	R	816	743–904
21	Tyndall	CHPS	Aniya (1995)	−51.6	R	1226	1145–1308
21	Tyndall	CHPS	Aniya (1995)	−51.6	R	1193	1091–1288
22	Lengua	Gran Campo Nevado	Koch and Killian (2005)	−53.0	T	322	–
22	Lengua	Gran Campo Nevado	Koch and Killian (2005)	−53.0	T	77	–
22	Lengua	Gran Campo Nevado	Koch and Killian (2005)	−53.0	T	64	–
22	Lengua	Gran Campo Nevado	Koch and Killian (2005)	−53.0	T	48	–
22	Lengua	Gran Campo Nevado	Koch and Killian (2005)	−53.0	T	38	–
22	Lengua	Gran Campo Nevado	Koch and Killian (2005)	−53.0	T	9	–

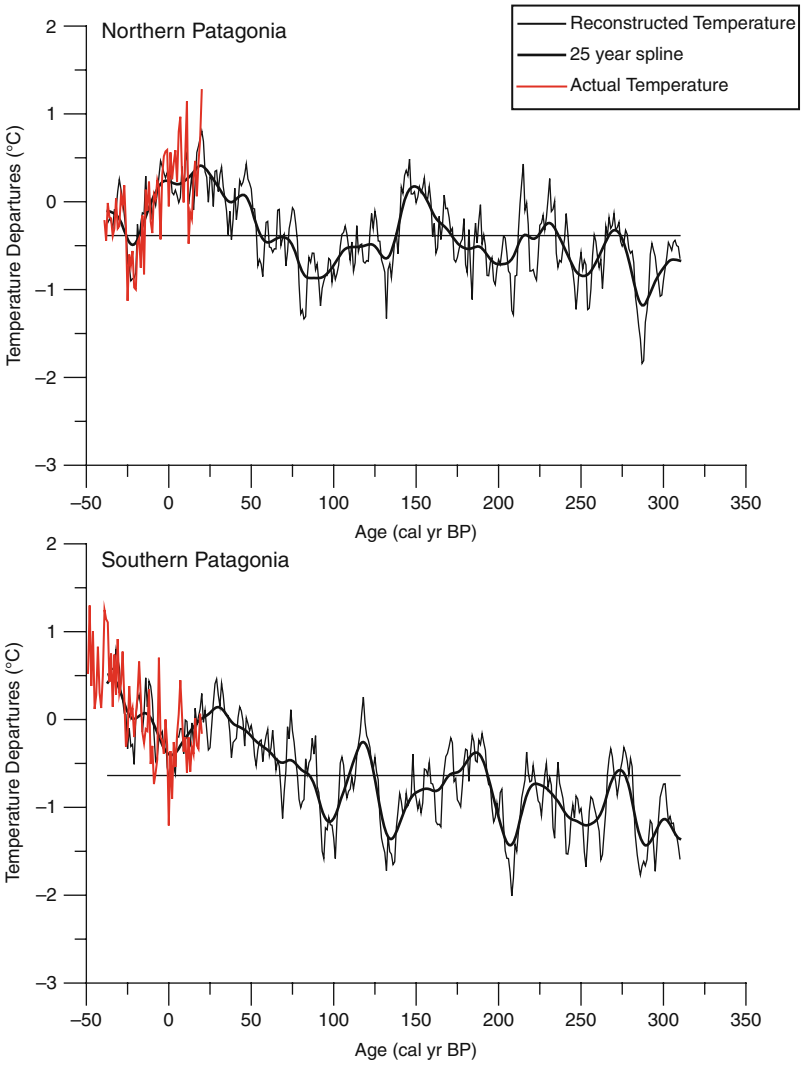

Fig. 15.8 Villalba et al. (2003) tree-ring derived temperature reconstruction for northern and southern Patagonia during the last four centuries derived from upper treeline locations (Fig. 15.1). The annually resolved temperature reconstructions are displayed along with a 25-year spline (*heavy dark lines*), and actual temperatures (*red lines*) from meteorological stations. The horizontal line represents the reconstructed mean. Both temperature reconstructions show a positive trend in temperature over the last 300 years, but there are differences in the timing of decadal variations and the short-term trend in temperature over the last ~50 years

we show the results from the northern and southern Patagonian tree-ring networks. There are some important similarities and differences between the two locations: although there is a clear positive trend in temperature between 1850 and 1920, the two records diverge (as does the instrumental record) during the last 50 years. In

addition, some of the multi-decadal variability observed in the records is not temporally consistent between northern and southern Patagonia. Some of the differences may be related to the different climatic forcing mechanisms between these two sites. When the northern Patagonia time series is regressed onto SST fields in the southern Pacific and the Atlantic basins, the variability is most strongly correlated with tropical and subtropical SST variability and is similar to the spatial SST structure of the PDO. In contrast, temperature variability in southern Patagonia is related to SST variability in the southern Atlantic Ocean and when regressed on a global field, the spatial structure is similar to the global warming mode of SST (Villalba et al. 2003). The Villalba et al. (2003) temperature reconstruction highlights three important points for our understanding of climate change in southern South America: (1) the period from 1850 to 1875 (100 to 75 cal year BP) marks a turning point in which temperatures begin to climb towards present day values, (2) the temperatures observed within the last 50 years are unprecedented with respect to the last 350 years (Villalba et al. 2003), (3) the multi-decadal temperature variations observed in the Northern Patagonia tree-ring reconstruction corresponds with detailed records of Frías glacier retreat rate (41°S), re-emphasizing the role temperature plays in controlling ice extent in Patagonia (Villalba et al. 2005).

In northern Patagonia, Villalba et al. (1990 and 1994) reconstructed summer temperature variations from a network of sites located in the Río Alerce valley in Argentina (∼41°S). The ∼1200 year reconstruction reveals two relatively cool periods from 1050 to 880 cal year BP and from 680 to 290 cal year BP with an intervening warm period between 870 and 700 cal year BP. The decadal variability in this record is similar to winter precipitation reconstructed from central Chile where warm summers in northern Patagonia correspond with wet winters in central Chile (Boninsegna 1990). Villalba (1994) interprets the consistency of the records as a shared response to ENSO variability during the last millennium.

Recent work by Villalba et al. (2008) has reconstructed past variations in the SAM index using tree-ring chronologies from a network of temperature- and precipitation-sensitive sites in Tasmania, New Zealand, and southern South America. Depending on which season is considered, the reconstructed record captures 47–51% of the total variance in the instrumental SAM index. The most significant result of the reconstruction is the large departure in SAM index values that begins in 1950 and extends to present day, which reflects the shift toward the positive phase of the SAM observed in instrumental records. The 1950 shift reflects the beginning of a major reorganization of atmospheric circulation in the high southern latitudes that is unprecedented within the last 350 years of the reconstruction (Villalba et al. 2008).

15.7 Marine Records

Marine sediment records from the Chilean continental shelf offer a unique opportunity to track changes in oceanic circulation and the response of continental weathering to atmospheric circulation. Lamy et al. (2001) and Lamy et al. (2002)

document changes in sea surface temperature (SST), sea surface salinity (SSS), productivity and precipitation-induced runoff during the last ~8000 cal year BP using a sediment core collected from the Chilean continental shelf at 41°S (Fig. 15.1). Combined alkenone and stable isotope analyses identified an overall decline in SST (~1°C) and SSS (~1 PSU) during the last 2000 years. This decline is coincident with an increase in biogenic opal and wt.% C, which was interpreted as an increase in productivity (Fig. 15.9). To investigate changes in weathering related to precipitation, Lamy et al. (2001) examine the Fe content of the bulk sediment and suggest that higher iron contents in the offshore core reflects greater erosion and runoff in the high Andes, where volcanic source rocks have high Fe content. Reduced Fe content in the sediment core is attributed to sediment derived from mixed sources including the Andes and the Chilean Coastal Range, the latter having relatively low Fe and apparently more sensitivity to rainfall variations than the Andes. Low Fe content in the sediment core is evidence of northward-shifted westerlies that enhanced precipitation in the Coastal Range and effectively diluted the contribution of the Andean source rocks, whereas high Fe content is attributed to a southward-shifted westerlies and a larger contribution of Andean-sourced sediment. Clay mineralogy was used to further this hypothesis. From the Fe profile, the Authors interpret significant changes in rainfall during the mid to late Holocene. Higher Fe counts centered at ~1700 and 700 cal year BP suggest reduced precipitation and southward-shifted westerlies, and two intervening periods centered on 1200 and 300 cal year BP imply northward shifted westerlies and increased precipitation on the continent east of the sediment core location. Lamy et al. (2001) identify arid and southward-shifted westerlies during the MCA (~700 cal year BP) and cooler and equatorward-shifted westerlies during the LIA (~300 cal year BP). Taken together, Lamy et al. (2002) argue that the declining SST, SSS, and Fe concentration at the coring site during the last 2000 years indicates an overall northward extension of the Antarctic Circumpolar Current and the westerlies.

Farther to the south (44°S), Mohtadi et al. (2007) use a similar suite of marine proxies to identify a northward shift in water mass properties (hydrography) and atmospheric circulation related to the westerlies and the Antarctic Circumpolar Current (ACC) between 1300 and 750 cal year BP. The 2° shift in latitude is associated with an overall decline in SST and SSS and increases in diatom concentration and the $\delta^{13}C$ of foraminifera. Taken together, Mohtadi et al. (2007) argued that the northward migration of cooler water and enhanced runoff from westerly-derived precipitation increased productivity between 1300 and 750 cal year BP

Fig. 15.9 (continued) inferred from the Fe profile. Higher Fe counts centered at ~1700 and 700 cal year BP are interpreted as reflecting reduced precipitation and southward-shifted westerlies, while two intervening periods centered on 1200 and 300 cal year BP suggest northward shifted westerlies and increased precipitation. Triangles at the top and at the base of the plot refer to median calibrated radiocarbon ages used in the GeoB 7186-3 and the GeoB 3313-1 chronologies

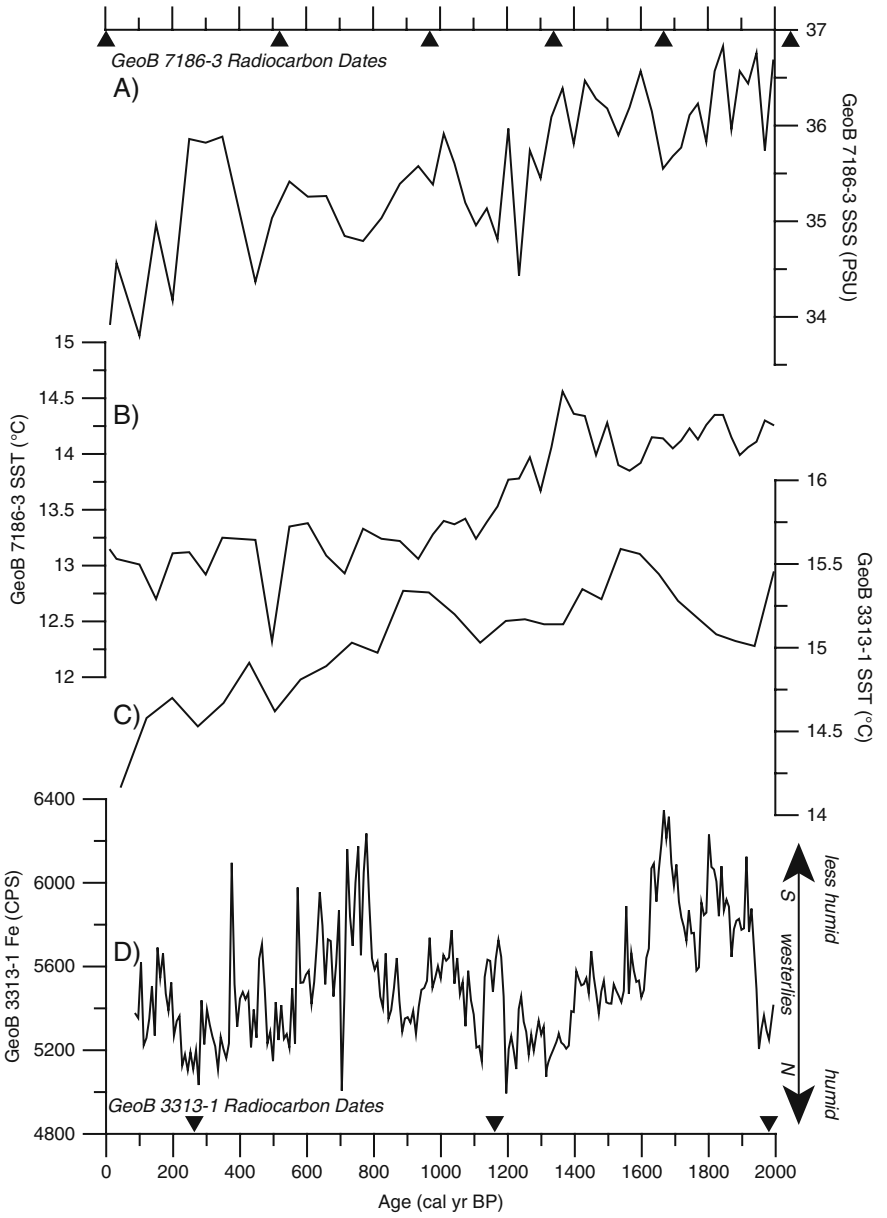

Fig. 15.9 Compilation of marine paleoclimate records from the Chilean continental shelf during the last 2000 years. (**A**) Alkenone-based sea surface salinity (SSS) and (**B**) sea surface temperature (SST) from core GeoB 7186-3 (44°S) (Mohtadi et al. 2007). (**C**) Alkenone-based SST reconstruction and (**D**) Fe content from core GeoB 3313-1 (41°S) (Lamy et al. 2001, Lamy et al. 2002). The SST and SSS reconstructions show an overall decline in sea surface temperature (SST) and sea surface salinity (SSS) that together have been interpreted to reflect a northward migration in the ACC during the last 2000 years. Changes in continental weathering related to westerly precipitation are

and further argued that the northward migration in the westerlies and the ACC is the result of a period of more La Niña-like conditions in the tropical Pacific Ocean.

15.8 Summary and Directions for Future Research

Understanding the last 2000 years of climate variability in southern South America is important because it provides information on processes influencing climate in the mid-latitudes of the Southern Hemisphere and enables us to place the rapid climate changes at present within a broader context. Over the last decade, numerous studies suggest that the southern westerlies play a role in the global carbon cycle, largely through air-sea gas exchange in the Southern Ocean, (Le Quéré et al. 2007, Lovenduski et al. 2007, Sigman and Boyle 2000, Toggweiler et al. 2006). Furthermore, increased atmospheric greenhouse gases in recent decades may at least be partly responsible for the tendency toward the positive phase of the SAM and increasing westerly wind intensity over the Southern Ocean (Kushner et al. 2001, Stone et al. 2001). Paleoclimate studies from southern South America offer one of the best opportunities to gain a better understanding of the natural processes influencing the strength and position of the southern westerlies because such data extend beyond the short record provided by instrumental and reanalysis data sets. In this section we summarize important aspects of climate variability during the last 2000 years in southern South America and highlight relevant paleoclimate records in Fig. 15.10.

1) The modern interannual climate variability, as revealed by instrumental and reanalysis data sets, is influenced by large-scale climate phenomena that originate in the high latitudes (SAM) as well as the tropics (ENSO). The apparent coupling between ENSO and the SAM (Fogt and Bromwich 2006, L'Heureux and Thompson 2006), influences teleconnections, and therefore, the overall climate system response in southern South America. The correlation between precipitation and the zonal winds is generally strong in southern South America and offers an important tool for reconstructing past variability in the wind field using paleoenvironmental records. However, the topography of the Andes and potential advection of moisture from the Atlantic produce heterogeneities in the precipitation-atmospheric circulation relationship in some areas in Southern Patagonia that bears further investigation.
2) Lacustrine sediment records provide continuous high-resolution time series that can be used to infer past variability of the westerlies with centennial- to millennial-scale resolution. Isotopic records from closed-basin lakes, in particular, are sensitive to changes in moisture balance, and when combined with other proxy data, can yield information regarding effective moisture and westerly wind strength. The late-Holocene record from Lago Guanaco in SW Patagonia, for example, suggests a significant increase in atmospheric circulation during the

last few hundred years, i.e., the LIA time in the Northern Hemisphere. Additional lacustrine records from Potrok Aike and Lago Cardiel all point toward increased variability in moisture balance/lake levels during the last 2000 years. Comparing the Guanaco and Potrok Aike records show consistent dry and wet intervals that are associated with the MCA and the LIA, respectively.

3) Radiocarbon-dated glacial deposits, primarily associated with outlet glaciers from the Northern and Southern Patagonian icefields, provide evidence for changes in glacial ice extent during the last two millennia. Holocene glacier records are hampered by a lack of chronologies and existing ages are spatially sporadic and often only provide "minimum- or maximum-limits". Taken at face value, a compilation of radiocarbon dates from the margins of the two ice sheets indicate expanded ice at ~1200 and ~600 cal year BP and more than once during the last 400 years. The pollen record from Lago Guanaco indicates that the millennial-scale variations in late Holocene ice extent observed in southern Patagonia glacier records are related to the overall strength of the westerlies at the latitude of the lake (51°S) (Moreno et al. 2009). Owing to its location in the lowlands directly east of the Andes, the Lago Guanaco record monitors past changes in the forest-steppe ecotone, which responds primarily to changes in precipitation of westerly origin. As pointed out by Moreno et al. 2009, the palynological evidence cannot exclude the likely possibility that increases in westerly wind variability were coincident with reductions in temperature. Tree-ring ages from moraines in Patagonia indicate, on average, ice retreat occurring since the late 19th century positions or LIA time. The most extensive ice advance of the mid- to late Holocene occurred at the start of Neoglaciation, ~5400 cal year BP. Mercer (1970) pointed out the trend of ice extent has decreased in South America during the Neoglacial. Patagonian glaciers responded primarily to temperature and secondarily to precipitation (e.g., Rignot et al. 2003, Cassasa 2003). Thus, future studies can maximize insight into former Patagonian climate by combining glacial changes with other precipitation sensitive proxies (e.g., pollen and isotopes), and tree-ring research.
4) Tree-rings offer excellent potential to investigate interannual to decadal variations in climate, and modern calibration with instrumental records allow the quantification of the magnitude of temperature and precipitation changes during the last millennium. Patagonian tree ring records provide evidence for warm dry conditions during the MCA centered between 870 and 700 cal year BP. Temperature reconstructions from northern and southern Patagonia indicate that 1850 to 1875 (100–75 cal year BP) marks an important turning point after which temperatures begins to climb towards present day values. In addition, temperature and atmospheric circulation as revealed in the reconstructed SAM index, indicates that the last 50 years are unprecedented within the context of the last 350 (Villalba et al. 2003).
5) Marine records from the Chilean continental shelf provide evidence of changes in ocean hydrography and productivity, in addition to, providing a monitor of terrestrial run-off related to westerly-derived precipitation. A Holocene record

obtained from ~41°S indicates declining SST and SSS, in combination with increased continental run-off during the last 2000 years (Lamy et al. 2001, Lamy et al. 2002). The Authors interpret these changes as a northward shift in both the westerlies and the ACC, which decreased SST and increased productivity through the delivery of nutrient-rich waters and the introduction of micronutrients from continental run-off. The marine records are important for our understanding of climate change in southern South America because they best illustrate the latitudinal coupling of SST gradients in the subtropical Pacific with latitudinal variations in atmospheric circulation (the westerlies).

We have assembled in Fig. 15.10 the proxy records that best summarize the key aspects of climate change in southern South America and address the research questions presented in the introduction of this chapter. Multiple paleoclimate archives from southern South America indicate an overall decrease in temperature and increase in westerly wind intensity during the last 2000 years that culminates between 400 and 50 cal year BP or European LIA time (Fig. 15.10). The marine records from the Chilean continental shelf document a ~1.5°C (Lamy et al. 2001) and a ~1°C (Mohtadi et al. 2007) SST cooling since 2000 cal year BP that culminates within the last 100 years (Fig. 15.10) that is interpreted as a northward shift in the Antarctic Circumpolar Current. Lake sediment records from southern Patagonia (Guanaco and Potrok Aike) and long tree-ring temperature reconstructions from northern Patagonia document aridity and warmer temperatures, respectively, between 900 and 700 cal year BP that is generally coincident with the timing of the MCA. The pollen and isotopic records from Guanaco indicate a significant increase in westerly wind strength within the last 2000 years that is coincident with the LIA. The culmination in strength in Lago Guanaco is similar in timing to the Siple

Fig. 15.10 Summary of paleoclimate records from southern South America and Antarctica. (**A**) Alkenone-based SST reconstruction from the Chilean continental shelf in northern Patagonia 45°S (Mohtadi et al. 2007). (**B**) Southern Patagonia 25-year spline tree-ring temperature reconstruction and actual temperature (*red line*) from Villalba et al. (2003). The horizontal line represents the reconstructed mean. Coldest reconstructed temperatures occur at the oldest part of the reconstruction (300–350 cal year BP) and increase abruptly after 100 cal year BP. (**C**) Fe record from the Chilean continental shelf reflecting changes in westerly-derived precipitation (Lamy et al. 2001). (**D**) Bivalve $\delta^{18}O$ (Moy et al. 2008) and (**E**) *Nothofagus*/Poaceae paleovegetation index (Moreno et al. 2009) from Lago Guanaco showing changes in evaporation and westerly-derived precipitation. Peak paleovegetation index and $\delta^{18}O$ values occur during LIA time (~400–100 cal year BP). (**F**) First EOF of Siple Dome Na^+ (Kreutz et al. 1997) calculated using a 25- (*solid line*) and 115-year (*dashed line*) window. Na^+ values culminate over a 300 year period centered on 200 cal year BP similar to the paleoclimate proxies from Lago Guanaco. The three vertical blue bars reflect periods of increased ice extent in CHPN, CHPS, and northern Patagonia glaciers identified in Fig. 15.7. The red rectangle labeled "1" refers to period of warm reconstructed summer temperatures in northern Patagonia (Villalba 1994) and the red rectangle labeled "2" indicates timing of drought termination in southern Patagonia (Stine 1994) and both events are generally coincident with inferred aridity and reduced westerlies from Lago Guanaco (**D**) and the Fe record from GeoB 3313-1 (**C**) and represents the MCA in Patagonia

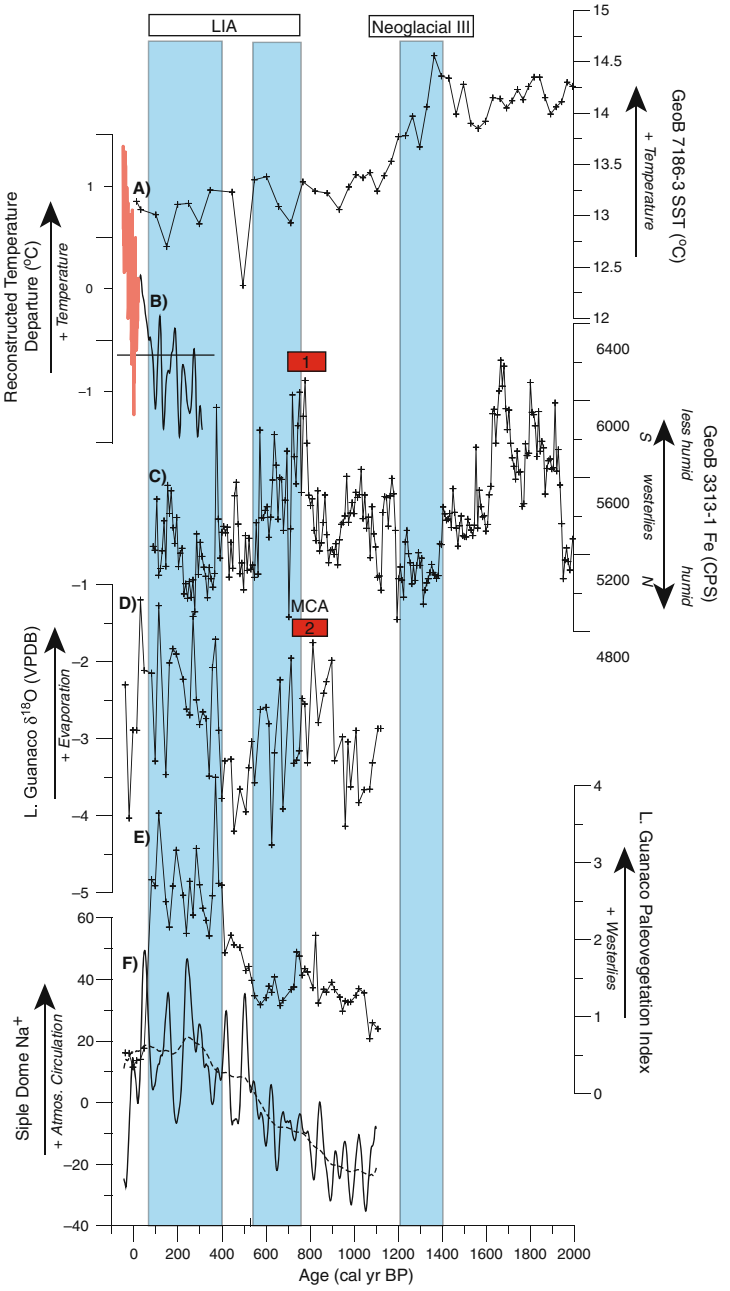

Fig. 15.10 (continued)

Dome record, indicating that atmospheric circulation increased throughout the high southern latitudes from 400 to 50 cal year BP. Tree ring records from northern and southern Patagonia indicate a shift towards warmer temperatures that begins at 1875 AD, is cotemporaneous with ice retreat from LIA ice positions, and represents the inception of warmer temperatures in southern Patagonia that exceed reconstructed temperatures during the last 350 years.

Future paleoclimate research in southern South America can work towards improving our current understanding of past climate and ecological change. The incorporation of new analytical techniques for proxy development and chronology refinement, in addition to, regional-scale multi-proxy reconstructions can significantly contribute to our understanding of past climate change. Chronologies can be improved by incorporating more high-quality radiocarbon dates from resistant and relevant organic fractions such as pollen and charcoal. Higher quality radiocarbon chronologies will facilitate comparisons with other paleoclimate records and provide a better understanding of the timing and variability of past climate change. Similarly, improved cosmogenic dating techniques can be further applied to Holocene glacial deposits (e.g., Schaefer et al. 2009). Marine paleoclimate records must apply a reservoir age correction to radiocarbon dates to account for the difference in ^{14}C content between the surface water and the atmosphere at a given location. The correction is often assumed to be constant over long periods of time (e.g. Holocene and late glacial timescales) despite evidence for significant changes in ocean circulation that would work to alter the past surface water ^{14}C content. Relatively new methods that measure ^{226}Ra in barite (van Beek et al. 2002), which as an independent chronometer, can be used in conjunction with radiocarbon dates to get a better understanding of past Holocene reservoir ages. The application of this technique along the Chilean continental margin could vastly improve marine chronologies and make them directly comparable to terrestrial records. The incorporation of relatively new isotopic and geochemical proxies for lake settings, such as the δD of terrestrial leaf waxes (Huang et al. 2002, Huang et al. 2004) and the TEX_{86} paleotemperature proxy (Tierney et al. 2008) can be combined and used to deconvolve seasonal variations in moisture balance and quantify past changes in temperature. However, modern calibration studies, that have yet to be undertaken in Patagonia, are required in order for these new methods to be interpreted correctly. Finally, multi-proxy regional reconstructions that combine multiple paleoclimate data sets from climatically relevant areas such as the Long-Term climate REconstruction and Dynamics of (southern) South America project (LOTRED) can be used to better understand past variations in climate. This project aims to build a database of paleoclimate proxy data from southern South America for the last 2000 years and to use these data to reconstruct past climate variability along multiple spatial and temporal scales.

Acknowledgments C. Moy acknowledges support from a U.S. State Department Fulbright to Chile, Department of Energy Global Change Education Program Graduate Fellowship, and a Stanford School of Earth Sciences McGee grant. P.I. Moreno acknowledges support from the Institute of Ecology and Biodiversity P05-002, contract PFB-23 and Fondecyt # 1040204, 1070991, and

1080485. T. Haberzettl acknowledges the support provided by Le Fonds québécois de la recherche sur la nature et les technologies (FQRNT). Helpful discussions with Rene Garreaud significantly improved the quality of this manuscript. We thank Andres Rivera for providing precipitation data from I. Evangelistas, which was collected by the Servicio Hidrográfico de la Armada de Chile (SHOA), and the Direccion General de Aguas (DGA) for the use of Torres del Paine meteorological data. We also thank Antje Schwalb and Cathy Whitlock for providing constructive reviews that greatly improved an earlier version of this manuscript. Figures 15.3 and 15.4 were constructed from NCEP-NCAR reanalysis data available at the NOAA/ESRL Physical Sciences Division, Boulder Colorado from their Web site at http://www.cdc.noaa.gov/. Southern South America base maps (Figs. 15.1, 15.3, and 15.7) were created using an online version of Generic Mapping Tools (GMT) at http://www.aquarius.ifm-geomar.de/.

References

Abarzua AM, Moreno PI (2008) Changing fire regimes in the temperate rainforest region of southern Chile over the last 16,000 yr. Quat Res 69:62–71

Aniya M (1988) Glacier inventory for the Northern Patagonia Icefield, Chile, and variations 1944/45 to 1985/86. Arc Antarct Alp Res 20:179–187

Aniya M (1995) Holocene glacial chronology in Patagonia: Tyndall and Upsala Glaciers. Arc Alp Res 27:311–322

Aniya M, Sato H, Naruse R et al (1996) The use of satellite and airborne imagery to inventory outlet glaciers of the Southern Patagonia Icefield, South America. Photogramm Eng Remote Sens 62:1361–1369

Anselmetti FS, Ariztegui D, de Baptist M et al (2009) Environmental history of Southern Patagonia unravelled by the seismic stratigraphy of Laguna Potrok Aike. Sedimentology 56:873–892

Aravena JC, Lara A, Wolodarsky-Franke A et al (2002) Tree-ring growth patterns and temperature reconstruction from Nothofagus pumillo (Fagaceae) forests at the upper tree line of southern Chilean Patagonia. Rev Chil Hist Nat 75:361–376

Auer V (1933) Verschiebungen der Wald-und Steppengebiete Feuerlands in postglazialer Zeit. Acta Geogr 5

Auer V (1958) The Pleistocene of Fuegopatagonia, part II: The history of the flora and vegetation. Ann Acad Sci Fenn 50:1–239

Bertrand S, Boes X, Castiaux J et al (2005) Temporal evolution of sediment supply in Lago Puyehue (Southern Chile) during the last 600 yr and its climatic significance. Quat Res 64:163–175

Boninsegna JA (1990) Santiago de Chile winter rainfall since 1220 as being reconstructed by tree rings. Quat South Am Antarct Peninsula 6:67–87

Bradley RS, Briffa KR, Cole J et al (2003) The climate of the last millennium. In: Alverson KD, Bradley RS, Pederson TF (eds) Paleoclimate, global change and the future. Springer-Verlag, New York, pp 105–141

Canadell JG, Le Quere C, Raupach MR et al (2007) Contributions to accelerating atmospheric CO2 growth from economic activity, carbon intensity, and efficiency of natural sinks. Proc Natl Acad Sci USA 104:18866–18870

Carrasco JF, Osorio R, Casassa, G (2008) Secular trend of the equilibrium-line altitude on the western side of the southern Andes, derived from radiosonde and surface observations. J Glaciol 54:538–550

Casassa G, Espizua L, Francau B et al (1998) Glaciers in South America. In: Haeberli W, Hoezle M, Suter S (eds) Into the second century of world wide glacier monitoring: Prospects and strategies. UNESCO Studies and Reports in Hydrology, Zurich, pp 125–146

Casassa G, Rivera A, Aniya M, Naruse R (2002) Current knowledge of the Southern Patagonian Icefield. In: Casassa G, Sepulveda FV, Sinclair RM (eds) The Patagonian Icefields: A

unique laboratory for environmental and climate change studies. Kluwer Academic/Plenum Publishers, New York, pp 67–83
Clapperton CM, Sugden DE (1988) Holocene glacier fluctuations in South America and Antarctica. Quat Sci Rev 7:185–198
Cobb KM, Charles CD, Cheng H, Edwards RL (2003) El Niño/Southern Oscillation and tropical Pacific climate during the last millennium. Nature 424:271–276
Dettman DL, Reische AK, Lohmann KC (1999) Controls on the stable Isotope composition of seasonal growth bands in fresh-water bivalves (unionidae). Geochimica et Cosmochimica Acta 63:1049–1057
Douglass DC, Singer BS, Kaplan MR et al (2005) Evidence of early Holocene glacial advances in southern South America from cosmogenic surface-exposure dating. Geology 33:237–240
Fey M, Korr C, Maidana NI et al (2009) Palaeoenvironmental changes during the last 1600 years inferred from the sediment record of a cirque lake in southern Patagonia (Laguna las Vizcachas, Argentina). Palaeogeography Palaeoclimatology Palaeoecology. (DOI:10.1016/j.palaeo.2009.01.012). Article in press; corrected proof available online (05/2009).
Fogt RL, Bromwich DH (2006) Decadal Variability of the ENSO Teleconnection to the high-latitude South Pacific governed by coupling with the southern annular mode. J Clim 19: 979–997
Galloway RW, Markgraf V, Bradbury JP (1988) Dating shorelines of lakes in Patagonia, Argentina. J South Am Earth Sci 1:195–198
Garreaud R (2007) Precipitation and circulation covariability in the extratropics. J Clim 20:4789–4797
Garreaud R, Vuille M, Compagnucci R, Marengo J (2008) Present-day South American Climate. Palaeogeography Palaeoclimatology Palaeoecology. (DOI:10.1016/j.palaeo.2007.10.032). Article in press; corrected proof available online (05/2009).
Garreaud RD, Aceituno P (2007) Atmospheric circulation over South America: Mean features and variability. In: Veblen T, Young K, Orme A (eds) The physical geography of South America. Oxford University Press, Oxford, England
Ghil MR, Allen M, Dettinger MD et al (2002) Advanced spectral methods for climatic time series. Rev Geophys 40:3.1–3.41
Gilli A, Anselmetti FS, Ariztegui DF et al (2001) Tracking abrupt climate change in the Southern Hemisphere: A seismic stratigraphic analysis of Lago Cardiel, Argentina (49°S). Terra Nova 13:443–448
Gilli A, Ariztegui D, Anselmetti FS et al (2005) Mid-Holocene strengthening of the Southern Westerlies in South America – Sedimentological evidences from Lago Cardiel, Argentina (49S). Glob Planet Change 49:75–93
Glasser NF, Hambrey MJ, Aniya M (2002) An advance of Soler Glacier, North Patagonian Icefield at c. AD 1222–1342. Holocene 12:113–120
Glasser NF, Harrison S, Winchester V, Aniya M (2004) Late Pleistocene and Holocene palaeoclimate and glacier fluctuations in Patagonia. Glob Planet Change 43:79–101
Haberzettl T, Corbella H, Fey M et al (2007) Lateglacial and Holocene wet-dry cycles in southern Patagonia: Chronology, sedimentology and geochemistry of a lacustine record from Laguna Portok Aike, Argentina. Holocene 17:297–310
Haberzettl T, Fey M, Lücke A et al (2005) Climatically induced lake level changes during the last two millennia as reflected in sediments of Laguna Potrok Aike, southern Patagonia (Santa Cruz, Argentina). J Paleolimnol 33:283–302
Haberzettl T, Kück B, Wulf S et al (2008) Hydrological variability in southeastern Patagonia and explosive volcanic activity in the southern Andean Cordillera during Oxygen Isotope Stage 3 and the Holocene inferred from lake sediments of Laguna Potrok Aike, Argentina. Palaeogeogr Palaeoclimatol Palaeoecol 259:213–229
Harrison S, Glasser N, Winchester V et al (2008) Glaciar León, Chilean Patagonia: Late-Holocene chronology and geomorphology. Holocene 18:643–652

Harrison S, Winchester V (1998) Historical fluctuations of the Gualas and Reicher Glaciers, North Patagonian Icefield, Chile. Holocene 8:481–485
Harrison S, Winchester V (2000) Nineteenth and twentieth century glacier fluctuations and climatic implications in the Arco and Colonia valleys, Hielo Patagónico Norte. Arct Antarct Alp Res 32:55–63
Harrison S, Winchester V, Glasser N (2007) The timing and nature of recession of outlet glaciers of Hielo Patagónico Norte, Chile, from their Neoglacial IV (Little Ice Age) maximum positions. Glob Planet Change 59:67–78
Heusser CJ (1966) Late-Pleistocene pollen diagrams from the Province of Llanquihue, southern Chile. Proc Am Philos Soc 110:269–305
Heusser CJ, Heusser LE (2006) Submillennial palynology and palaeoecology of the last glaciation at Taiquemo (similar to 50,000 cal yr, MIS 2–4) in southern Chile. Quat Sci Rev 25:446–454
Heusser CJ, Heusser LE, Lowell TV (1999) Paleoecology of the southern Chilean Lake District-Isla Grande de Chiloé during middle-Late Llanquihue glaciation and deglaciation. Geogr Ann Ser A Phys Geogr 81 A:231–284
Hodell DA, Kanfoush SL, Shemesh A et al (2001) Abrupt cooling of Antarctic surface waters and sea ice expansion in the South Atlantic sector of the Southern Ocean at 5000 cal yr B.P. Quat Res 56:191–198
Huang Y, Shuman B, Wang Y, Webb T (2002) Hydrogen isotope ratios of palmitic acid in lacustrine sediments record late Quaternary climate variations. Geology 30:1103–1106
Huang Y, Shuman B, Wang Y, Webb T (2004) Hydrogen isotope ratios of individual lipids in lake sediments as novel tracers of climatic and environmental change: A surface sediment test. J Paleolimnol 31:363–375
Huber UM, Markgraf V (2003) European impact on fire regimes and vegetation dynamics at the steppe-forest ecotone of southern Patagonia. Holocene 13:567–579
Jones JM, Widmann M (2004) Atmospheric science: Early peak in Antarctic oscillation index. Nature 432:290–291
Jones PD, Mann ME (2004) Climate over past millennia. Rev Geophys 42:1–42
Kalnay E, Kanamitsu M, Kistler R et al (1996) The NCEP/NCAR 40-year Re-analysis Project. Bull Am Meteorol Soc 77:437–471
Koch J, Killian, R (2005) 'Little Ice Age' glacier fluctuations, Gran Campo Nevado, southernmost Chile. Holocene 15:20–28
Kreutz KJ, Mayewski PA, Meeker LD et al (1997) Bipolar changes in atmospheric circulation during the little ice. Sci 277:1294–1296
Kushner PJ, Held IM, Delworth TL (2001) Southern Hemisphere Atmospheric Circulation Response to Global Warming. J Clim 14:2238–2249
Kwok R, Comiso JC (2002) Spatial patterns of variability in Antarctic surface temperature: Connections to the Southern Hemisphere Annular Mode and the Southern Oscillation. Geophys Res Lett 29:1–4
L'Heureux ML, Thompson DWJ (2006) Observed relationships between the El Niño–Southern Oscillation and the extratropical zonal-mean circulation. J Clim 19:276–287
Lamy F, Hebbeln D, Röhl U, Wefer G (2001) Holocene rainfall variability in southern Chile: A marine record of latitudinal shifts of the southern westerlies. Earth Planet Sci Lett 185:369–382
Lamy F, Ruhlemann C, Hebbeln D, Wefer G (2002) High- and low-latitude climate control on the position of the southern Peru-Chile Current during the Holocene. Paleoceanography 17:1028
Lara A, Aravena JC, Villalba R et al (2001) Dendroclimatology of high-elevation Nothofagus pumilio forests at their northern distribution limit in the central Andes of Chile. Can J For Res 31:925–936
Lara A, Villalba R (1993) A 3620-year temperature record from Fitzroya cupressoides tree rings in southern South America. Science 260:1104–1106
Lara A, Villalba R, Urrutia R (2008) A 400-year tree-ring record of the Puelo River summer-fall streamflow in the Valdivian Rainforest eco-region, Chile. Clim Change 86:331–356

Lawrence DB, Lawrence EG (1959) Recent glacier variations in southern South America. In: Technical Report, Office of Naval Research. American Geographical Society, New York
Le Quéré C, Rodenbeck C, Buitenhuis ET et al (2007) Saturation of the Southern Ocean CO2 Sink Due to Recent Climate Change. Science 316:1735–1738
Legates DR, Willmott CJ (1990) Mean Seasonal and Spatial Variability Global Surface Air Temperature. Theor Appl Climatol 41:11–21
Leng MJ, Marshall JD (2004) Palaeoclimate interpretation of stable isotope data from lake sediment archives. Quat Sci Rev 23:811–831
Lovenduski NS, Gruber N, Doney SC, Lima ID (2007) Enhanced CO2 outgassing in the Southern Ocean from a positive phase of the Southern Annular Mode. Glob Biogeochem Cycles 21:GB2026 1–14
Malagnino EC, Strelin, JA (1992) Variations of Upsala Glacier in southern Patagonia since the late Holocene to the present. In: Naruse R, Aniya M (eds) Glaciological researches in Patagonia, 1990. Japanese Society of Snow and Ice, Japan, pp 61–85
Markgraf V (1993) Paleoenvironments and Paleoclimates in Tierra-Del-Fuego and Southernmost Patagonia, South-America. Palaeogeogr Palaeoclimatol Palaeoecol 102:53–68
Markgraf V, Bradbury JP, Schwalb A et al (2003) Holocene palaeoclimates of southern Patagonia: Limnological and environmental history of Lago Cardiel, Argentina. Holocene 13:581–591
Marshall GJ (2003) Trends in the Southern Annualar Mode from observations and Reanalysis. J Clim 16:4134–4143
Matthews JA, Briffa KR (2005) The 'Little Ice Age': Re-evaluation of an evolving concept. Geogr Ann 87:17–36
Mayr C, Fey M, Haberzettl T et al (2005) Palaeoenvironmental changes in southern Patagonia during the last millennium recorded in lake sediments from Laguna Azul (Argentina). Palaeogeogr Palaeoclimatol Palaeoecol 228:203–227
Mayr C, Wille M, Haberzettl T et al (2007) Holocene variability of the Southern Hemisphere westerlies in Argentinean Patagonia (52°S). Quat Sci Rev 26:579–584
McCormac FG, Hogg AG, Blackwell PG et al (2004) SHCal04 Southern Hemisphere Calibration 0–11.0 cal kyr BP. Radiocarbon 46:1087–1092
Mercer JH (1965) Glacier variations in Southern Patagonia. Geogr Rev 55:390–413
Mercer JH (1968) Variations in some Patagonian glaciers since the late-glacial. Am J Sci 266: 91–109
Mercer JH (1970) Variations of some Patagonian glaciers since the Late Glacial: II. Am J Sci 269:1–25
Mercer JH (1976) Glacial history of southernmost South America. Quat Res 6:125–166
Mercer JH (1982) Holocene glacial variations in southern South America. Striae 18:35–40
Mo K (2000) Relationships between low-frequency variability in the southern hemisphere and sea surface temperature anomalies. J Clim 13:3599–3610
Mohtadi M, Romero OE, Kaiser J, Hebbeln D (2007) Cooling of the southern high latitudes during the Medieval Period and its effect on ENSO. Quat Sci Rev 26:1055–1066
Moreno PI (2004) Millennial-scale climate variability in northwest Patagonia over the last 15000 yr. J Quat Sci 19:35–47
Moreno PI, Francois JP, Villa-Martinez R, Moy CM (2009) Millennial-scale variability in Southern Hemisphere westerly wind activity over the last 5000 years in SW Patagonia. Quat Sci Rev 28:25–38
Moreno PI, Lowell TV, Jacobson GL, Denton GH (1999) Abrupt vegetation and climate changes during the last glacial maximum and last termination in the Chilean Lake District: A case study from Canal de la Puntilla (41 degrees s). Geogr Ann Ser A Phys Geogr 81A:285–311
Moy CM, Dunbar RB, Moreno P et al (2008) Isotopic evidence for hydrologic change related to the westerlies in SW Patagonia, Chile, during the last millennium. Quat Sci Rev 27: 1335–1349
Moy CM, Seltzer GO, Rodbell DT, Anderson DM (2002) Variability of El Niño/Southern Oscillation activity at millennial timescales during the Holocene epoch. Nature 420:162–165

Naranjo JA, Stern CR (1998) Holocene explosive activity of Hudson Volcano, southern Andes. Bull Volcanol 59:291–306
Naruse R (2006) The response of glaciers in South America to environmental change. In Knight P (ed) Glaciers and Earth's changing environment. Blackwell, Oxford, pp 231–238
Porter SC (2000) Onset of Neoglaciation in the Southern Hemisphere. J Quat Sci 15:395–408
Rabassa J, Brandani A, Boninsegna JA, Cobos DR (1984) Cronologia de la "Pequeña Edad del Hielo" en los glaciares Rio Manso y Castafio Overo, Cerro Tronador, Provincia de Rio Negro. 9no. Congreso Geologico Argentino Actas 3:624–639
Rein B, Luckge A, Sirocko F (2004) A major Holocene ENSO anomaly during the Medieval period. Geophys Res Lett 31:L17211 1–4
Rignot E, Rivera A, Casassa G (2003) Contribution of the Patagonia Icefields of South America to Sea Level Rise. Science 302:434–437
Rivera A, Benham T, Casassa G et al (2007) Ice elevation and areal changes of glaciers from the Northern Patagonia Icefield, Chile. Glob Planet Change 59:126–137
Rivera A, Casassa G (2004) Ice elevation, areal, and frontal changes of glaciers from national park Torres del Paine, Southern Patagonia Icefield. Arct Antarct Alp Res 36:379–389
Röthlisberger E (1986) 1000 Jahre Gletschergeschichte der Erde. Verlag Sauerlander, Salzburg
Schaefer JM, Denton GH, Kaplan MR et al (2009) High-frequency Holocene glacier fluctuations in New Zealand differ from the northern signature. Science 324:622–625
Schneider C, Geis D (2004) Effects of El Niño-Southern Oscillation on southernmost South America precipitation revealed from NCEP-NCAR reanalysis and weather station data. Int J Climatol 24:1057–1076
Schneider C, Glaser M, Kilian R et al (2003) Weather observations across the southern Andes at 53 °S. Phys Geogr 24:97–119
Sigman DM, Boyle EA (2000) Glacial/interglacial variations in atmospheric carbon dioxide. Nature 407:859–869
Stine S (1994) Extreme and persistent drought in California and Patagonia during mediaeval time. Nature 369:546–549
Stine S, Stine M (1990) A record from Lake Cardiel of climate change in southern South America. Nature 345:705–708
Stone, DA, Weaver AJ, Stouffer RJ (2001) Projection of climate change onto modes of atmospheric variability. J Clim 14:3551–3565
Strelin JA, Malagnino EC (2000) Late Glacial history of Lago Argentino, Argentina, and age of the Puerto Bandera moraines. Quat Res 54:339–347
Sweda T (1987) Recent retreat of Soler Glacier, Patagonia as seen from vegetation recovery. Bull Glacier Res 4:119–124
Szeicz JM, Haberle SG, Bennett KD (2003) Dynamics of North Patagonian rainforests from fine-resolution pollen, charcoal and tree-ring analysis, Chonos Archipelago, Southern Chile. Austral Ecol 28:413–422
Szeicz JM, Zeeb BA, Bennett KD, Smol JP (1998) High-resolution paleoecological analysis of recent disturbance in a southern Chilean Nothofagus forest. J Paleolimnol 20:235–252
Thompson DWJ, Solomon S (2002) Interpretation of recent Southern Hemisphere climate change. Science 296:895–899
Thompson DWJ, Wallace JM (2000) Annular modes in the extratropical circulation. Part II: Trends. J Clim 13:1018–1036
Tierney JE, Russell JM, Huang Y et al (2008) Northern Hemisphere Controls on Tropical Southeast African Climate During the Past 60,000 Years. Science 322:252–255
Toggweiler JR, Russell JL, Carson SR (2006) Midlatitude westerlies, atmospheric CO_2, and climate change during the ice ages. Paleoceanography 21:PA2005
Trenberth KE (1991) Storm Tracks in the Southern Hemisphere. J Atmos Sci 48:2159–2178
van Beek P, Reyss JL, Paterne M et al (2002) ^{226}Ra in barite: Absolute dating of Holocene Southern Ocean sediments and reconstruction of sea-surface reservoir ages. Geology 30:731–734

Villagrán C (1985) Análisis palinológico de los cambios vegetacionales durante el Tardiglacial y Postglacial en Chiloé, Chile. Revista Chilena de Historia Natural 58:57–69
Villagrán C (1988) Late Quaternary vegetation of Southern Isla Grande de Chiloé, Chile. Quat Res 29:294–306
Villalba R (1990) Climatic fluctuations in northern Patagonia during the last 1000 years as inferred from tree-ring records. Quat Res 34:346–360
Villalba R (1991) Latitude of the surface high-pressure belt over western South America during the last 500 years as inferred from tree-ring analysis. Quat South Am Antarct Peninsula 7:305–327
Villalba R (1994) Tree-ring and glacial evidence for the Medieval Warm Epoch and the Little Ice Age in southern South America. Clim Change 26, 183–197
Villalba R (2007) Tree-ring evidence for tropical-extratropical influences on climate variability along the Andes in South America. PAGES Newsl 15:23–25
Villalba R, Boninsegna JA, Lara A et al (2008) A dendrochronological approach to estimates of past changes in the Antarctic Oscillation. In: Documenting, understanding and projecting changes in the hydrological cycle in the American Cordillera, IAI CRN 2047, Second Science Meeting. San Carlos, Argentina
Villalba R, Lara A, Boninsegna JA et al (2003) Large-scale temperature changes across the southern Andes: 20th-century variations in the context of the past 400 years. In: Climatic change climate variability and change in high elevation regions: Past, Present and Future, 25–28 June 2001, vol 59. Davos, Switzerland, pp 177–232
Villalba R, Masiokas MH, Kitzberger T, Boninsegna JA (2005) Biogeographical consequences of recent climate changes in the Soutern Andes of Argentina. In: Huber UM, Bugmann HKM, Reasoner MA (eds) Global change and mountain regions: An overview of current knowledge. Advances in global change research. Springer, New York, 650 pp
von Grafenstein U, Erlenkeuser H, Trimborn, P (1999) Oxygen and carbon isotopes in modern fresh-water ostracod valves: Assessing vital offsets and autoecological effects of interest for paleoclimate studies. Palaeogeogr Palaeoclimatol Palaeoecol 148:133–152
Warren C, Sugden D (1993) The Patagonian icefields: A glaciological review. Arct Antarct Alp Res 25:316–331
Whitlock C, Moreno PI, Bartlein, P (2007) Climatic controls of Holocene fire patterns in southern South America. Quat Res 68:28–36
Wille M, Maidana NI, Schäbitz F et al (2007) Vegetation and climate dynamics in southern South America: The microfossil record of Laguna Potrok Aike, Santa Cruz, Argentina. Rev Palaeobot Palynol 146:234–246
Winchester V, Harrison S, Warren CR (2001) Recent retreat of Glaciar Nef, Chilean Patagonia, dated by lichenometry and dendrochronology. Arct Antarct Alp Res 33:266–273
Wolter K, Timlin MS (1993) Monitoring ENSO in COADS with a seasonally adjusted principal component index. In: N. NOAA/N MC/CAC (ed) Proceedings of the 17th Climate Diagnostics Workshop, Norman, OK, pp 52–57
Wolter K, Timlin MS (1998) Measuring the strength of ENSO events – how does 1997/98 rank? Weather 53:315–324
Xie P, Arkin PA (1997) Global Precipitation: A 17-year monthly analysis based on gauge observations, satellite estimates, and numerical model outputs. Bull Am Meteorol Soc 78:2539–2558